

was chosen as a reference gene. Every reaction was triplicated. CopyCaller Software v2.0 (Applied Biosystems) was used to determine the copy number status of each target region.

2.6. Targeted capture and massive parallel sequencing

We conducted exome analysis on one affected family member who was negative for mutations in the exons of the 6 MODY genes. We targeted all protein-coding regions as defined by RefSeq37. Approximately 210,000 coding exons from 3 µg of genomic DNA were captured using the Agilent SureSelect Human All Exon 50 Mb kit, following the manufacturer's protocols. The whole-exome DNA library was sequenced on an Illumina Genome Analyzer Ix in 76-bp paired-end reads using two channels. Sequence reads were mapped to the reference human genome (Ghr37/hg19) using the Burrows-Wheeler Aligner (<http://bio-bwa.sourceforge.net/>). Variant detection was performed with the CASAVA software (version 1.7; Illumina). Calls of variants were filtered to include only those with $\geq 8\times$ coverage, ≥ 40 consensus quality and ≥ 20 mapping quality.

2.7. Genotyping of SNPs

Genotyping of variants identified in the exome sequencing was performed in 105 normoglycemic controls and 67 lean diabetes subjects. The PCR-restriction fragment length polymorphism method for p.A80T of *CENPH*, p.R29C of *SREK1IP1*, and p.S33G of *SMAGP* and the Taqman method (Applied Biosystems) for p.F120L of *TMEM174*, p.P1818L of *NACA*, p.N1072K of *EEA1*, and p.E361G of *LRR1Q1* were used. Genotyping of the p.N1072K variant of *EEA1* was performed in another, unrelated 64 familial diabetes subjects.

2.8. RT-PCR analysis of the *TMEM174* gene product in mouse tissues

Pancreatic islets and tissues of the lung, the heart, the liver and the kidney were obtained from C57BL/6 mice. Complementary DNA was prepared by reverse transcriptase (Invitrogen) with an oligo(dT) primer (Invitrogen). Messenger RNA expression was examined by PCR using the LA Taq (TaKaRa) and the oligonucleotide primers. Thermal cycling conditions were denaturation at 95 °C for 10 min followed by 35 cycles at 95 °C for 15 s and 58 °C for 1 min. C- and N-terminal primers of target molecules were designed as follows: GAPDH forward, 5'-aatggtgaaggtcgggtg-3', and reverse, 5'-tcgttgatggcaacaatc-3'; and *TMEM174* forward, 5'-taccctcaagacaatgctg-3', and reverse, 5'-tggaggagaaacatacga-3'.

2.9. Statistical analysis

Frequencies of nucleotide changes in normoglycemic controls and lean diabetes subjects were compared by the Pearson's chi-squared test or the Fisher's exact test, wherever appropriate.

2.10. Ethics

Ethical approval for this study was given by the Institutional Review Board and Ethics Committee of Kyoto University School of Medicine, Kyoto University, Japan (approval number: G267; approval date: 9 October 2008). Written, informed consent was obtained from each participant. This study was carried out in accordance with the Declaration of Helsinki as revised in 2000.

3. Results

3.1. Characteristics of family members

A family with a 3-generation history of diabetes was enrolled in this study (Fig. 1, Table 1). Thirteen members (6 men, 7 women)

had previously been diagnosed with diabetes, 9 of them before the age of 40. Nine of the 13 family members with diabetes were lean (BMI < 25); none of them were both obese and late-onset (later than 40). Eight family members were treated with oral antidiabetic drugs and 1 with insulin.

3.2. Detection of a diabetes susceptibility mutation in the hepatocyte nuclear factor 4 alpha (*HNF4A*) gene

For the index case, we performed direct sequencing in entire coding exons of the 6 MODY genes. The detected missense SNPs were the p.S487N variant of *HNF1A* (rs2464196) and the p.T130I variant of *HNF4A* (rs1800961) (Supplementary Table 3). The p.T130I variant of *HNF4A* was not a cause of MODY but was associated with late-onset type 2 diabetes in a previous report [13], so we genotyped all family members for the variant. As a result, 6 members with diabetes and 1 member without diabetes were found to be heterozygous for the variant (Fig. 1). We hypothesized that the disease susceptibility variant for the 6 members with diabetes was the p.T130I variant of *HNF4A*. We detected no copy number losses in *HNF1A*, *HNF1B*, and *GCK* on the index case (Supplementary Table 4).

3.3. Linkage analysis

We performed linkage analysis to identify the susceptibility gene in the family members with diabetes and also negative for the p.T130I variant of *HNF4A*. Family members positive for the variant were assigned as having unknown phenotype in the linkage analysis. A total of 12 family members (7 assigned as having affected phenotype, 4 assigned as having unknown phenotype, and 1 assigned as having unaffected phenotype) were included in the linkage analysis, assuming an autosomal dominant model. The genome-wide linkage results in the screening are shown in Fig. 2. Regions of potential interest by the multipoint LOD score were observed on chromosomes 4, 5 and 12. After fine mapping, 4q34, 5q11–q13, and 12p11–q22 were revealed to be candidate regions (Supplementary Table 5, LOD = 1.80).

3.4. Candidate variants in exome sequencing

We searched candidate genetic variants in the implicated linkage region by performing exome sequencing in family member II-2, who was negative for mutations in the exons of the 6 MODY genes. Family member II-2 was also negative for copy number losses in *HNF1A*, *HNF1B*, and *GCK* (Supplementary Table 4). The exome DNA library of the family member was sequenced in 76 bp paired-end reads, using 2 channels of Genome Analyzer Ix. We generated approximately 153 million reads and 98.02% of the reads were mapped to the reference human genome (Ghr37/hg19). On target rate to the bait was 59.1% and coverage depth was ≥ 3 in 97.40% of the targeted region and ≥ 20 in 87.11% of the targeted region. We predicted that the familial clustering of diabetes is caused by a rare non-synonymous variant, and focused our analysis on

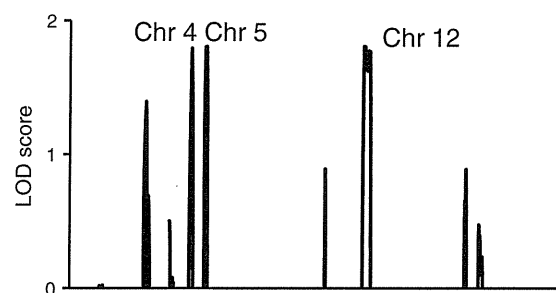


Fig. 2. Multipoint LOD scores in the genome-wide linkage analysis for the pedigree.

non-synonymous heterozygous or homozygous variants absent in the dbSNP131 (<http://www.ncbi.nlm.nih.gov/projects/SNP/>). In the implicated linkage region, we detected 10 such variants. All of these variants were heterozygous and were validated by Sanger method (Table 2). We genotyped all family members included in the linkage analysis for the 10 variants and 7 of them were detected in all affected family members without the p.T130I variant of *HNF4A*.

3.5. Allele frequencies of the candidate variants in cases and controls

To determine whether each of the 7 variants was rare or common in the general Japanese population without hyperglycemia, we genotyped 105 normoglycemic controls for the 7 variants. Minor allele frequencies ranged from 0.0% to 4.7% for the 7 variants (Table 3). We then genotyped 67 lean diabetes subjects to determine the frequency of the variants in a group predicted to be genetically predisposed to diabetes. The p.N1072K variant of *EEA1* was found to be significantly more frequent in the lean diabetes subjects than in the normoglycemic controls (0 in normoglycemic controls, 4 in lean diabetes subjects, $p = 0.022$, Fisher's exact test). Two of the 4 lean diabetes subjects had family history; the mother of one subject and a sibling of the other subject had diabetes, but DNA samples of their family members were unavailable. We also genotyped the p.N1072K variant of *EEA1* in another, unrelated 64 familial diabetes subjects and found 3 of them to be heterozygous for the variant; the minor allele frequency being 3/128 (2.3%). For 1 of the 3 subjects heterozygous for the variant, a DNA sample of a family member was available and the variant was concordant with the affection status in the family (Supplementary Fig. 1, Supplementary Table 6).

3.6. Linkage reanalysis of the family with a 3-generation history of diabetes

We performed a linkage analysis in the family with a 3-generation history of diabetes of chromosome 12 using the g.93175846 genotype in *EEA1* together with the microsatellite markers. We reassigned the affection status: subjects heterozygous for the p.N1072K variant of *EEA1* (II-1, II-2, II-4, II-5, II-6, II-7, III-1, III-2, and III-4) were considered as having affected phenotype and subjects negative for the variant (II-9 and III-3) were considered as having unaffected phenotype. We found a LOD score of 2.70 at the locus of the p.N1072K variant of *EEA1* (Fig. 3).

4. Discussion

In the present study, we analyzed a family with highly aggregated diabetes mellitus by combining exome sequencing and a linkage analysis. We identified a candidate susceptibility variant of *EEA1* in the linkage region located on chromosome 12p11–q22. The region has not been reported in previous linkage analyses with familial diabetes in Japan.

Table 2
Non-synonymous nucleotide changes in the linkage regions.

Gene	Chr:position (GRCh37) nucleotide change	Amino acid change	Concordance
SREK11P1	5:64037004 G>A	R29C	+
CENPH	5:68490521 G>A	A80T	+
TMEM174	5:72469428 T>C	F120L	+
SMAGP	12:51640553 T>C	S33G	+
KRT78	12:53233268 C>T	M424I	–
NACA	12:57109861 G>A	P1818L	+
LRIG3	12:59274465 G>A	R567W	–
TMEM19	12:72092800 C>T	P253L	–
LRRIQ1	12:85449653 T>C	E361G	+
EEA1	12:93175846 A>T	N1072K	+

Table 3
Allele frequencies of candidate variants in the normoglycemic controls and the lean diabetes subjects.

Gene	Amino acid change	Detected number of alleles					
		Controls (n = 105)			Diabetes (n = 67)		
		Major	Minor	MAF	Major	Minor	MAF
SREK11P1	R29C	200	10	0.047	126	8	0.059
CENPH	A80T	208	2	0.009	132	2	0.014
TMEM174	F120L	210	0	0.000	134	0	0.000
SMAGP	S33G	208	2	0.009	134	0	0.000
NACA	P1818L	204	6	0.029	134	0	0.000
LRRIQ1	E361G	209	1	0.004	132	2	0.014
EEA1	N1072K	210	0	0.000	130	4 ^a	0.029

MAF = Minor Allele Frequency.

^a Fisher's exact test, $p < 0.05$.

The *EEA1* variant was detected in all affected family members without the p.T130I variant of *HNF4A*. We validated the candidate susceptibility variant of *EEA1* by performing a case–control study. The variant was significantly more frequent in the diabetes subjects than in the cohort of subjects that retained fasting normoglycemia for 5 years. It is important that the *EEA1* variant was not detected in 105 controls that are supposed to have protective genetic background against diabetes, because enough power to detect a polymorphism present in 1% of the control chromosomes was achieved by genotyping 105 individuals.

In several studies, exome sequencing has been performed to identify the cause of neonatal diabetes or familial diabetes and it has successfully identified the causal mutations in genes previously known to be involved in the pathogenesis of diabetes [14–17]. To our knowledge this is the first study to propose a new diabetes susceptibility gene by utilizing exome sequencing.

The *EEA1* protein is known to localize exclusively to early endosomes. *EEA1* is a membrane bound, endosome fusion promoting protein and an effector of the small GTPase Rab5 [18–20]. *EEA1* is a coiled-coil homodimer with an N-terminal C₂H₂ zinc finger and a C-terminal region containing a calmodulin binding motif and a FYVE domain [21]. It is reported that *EEA1* deficiency decreased insulin-stimulated glucose uptake and insulin-stimulated translocation of glucose transporter type 4 to the plasma membrane in human adipocytes [22]. Thus, the variant of *EEA1* could cause type 2 diabetes susceptibility by inducing insulin resistance. The Asn1024 residue of *EEA1* is conserved among mammals [23], suggesting that a substitution to lysine might affect the function of *EEA1*; however, the residue is located on the coiled-coil domain not directly involved in the interaction with Rab5 GTPase or endosomal membrane [21]. Further study is necessary to evaluate the functional significance of the variant.

Our study has other limitations. First, the p.T130I variant of *HNF4A* is not a cause of MODY and is reported to be found in non-diabetic individuals [13], so the possibility remains that the genetic cause of diabetes for

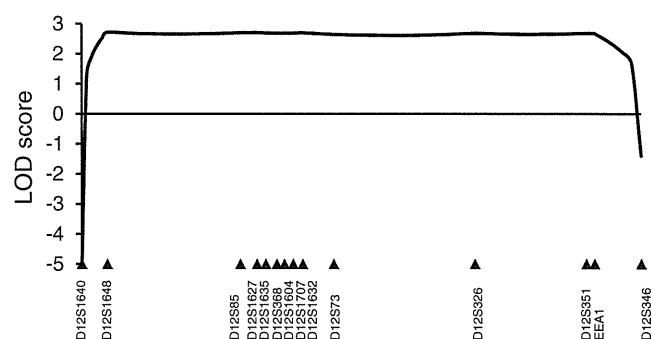


Fig. 3. Multipoint LOD scores for chromosome 12 after fine mapping and reassignment of the affection status.

members I-3, II-9, II-10, and III-3 in the family is not the p.T130I variant of *HNF4A*. Second, we focused only on nonsynonymous single nucleotide variants in the linkage region and eliminated a large number of insertion/deletions detected in the exome sequencing, most of which were not confirmed by the direct sequencing [24]. Third, in the linkage region, besides the p.N1072K variant of *EEA1*, p.F120L of *TMEM174* was also undetectable in the 105 control subjects and was considered rare. The p.F120L variant of *TMEM174* was not detected in the 67 diabetes subjects, but it might be an extremely rare diabetes susceptibility variant that is found specifically in this family. The PolyPhen-2 prediction score for the p.F120L variant of *TMEM174* was 0.990 and the variant was predicted to be probably damaging, and the p.T130I variant of *HNF4A* and the p.N1072K variant of *EEA1* were predicted to be benign with the prediction score of 0.001 and 0.191 respectively [25]. However, we thought that the *TMEM174* gene is less likely to be the cause of diabetes than the *EEA1* gene because the *TMEM174* gene is almost specifically expressed in the kidney [26], not in the pancreatic islets or the liver according to our RT-PCR analysis using mouse tissues (Supplementary Fig. 2). Fourth, the LOD score at the locus of the p.N1072K variant of *EEA1* in the linkage analysis was slightly lower than the genome-wide significance level. This lower-than-expected LOD score may be attributable to the difficulties inherent to the genetic heterogeneity of diabetes.

5. Conclusion

We propose that the *EEA1* gene is a candidate type 2 diabetes susceptibility gene. A family-based approach combined with exome sequencing may be a useful strategy to elucidate the complex genetic background of type 2 diabetes by identifying rare disease variants not detected by GWAS.

Supplementary data to this article can be found online at <http://dx.doi.org/10.1016/j.ymgme.2013.02.010>.

Acknowledgments

We thank K. Akitomo and S. Yasui for technical assistance. This work was supported by a grant for Research on Human Genome Tailor-Made from the Ministry of Health, Labor, and Welfare of Japan, a grant for Research on Drug Discovery Platform from the Ministry of Health, Labor, and Welfare of Japan, a grant for Intractable Disease Research Program from the Ministry of Health, Labor, and Welfare of Japan, Scientific Research Grants from the Ministry of Education, Culture, Sports, Science, and Technology of Japan, and a grant from Core Research for Evolutional Science and Technology (CREST) of Japan Science and Technology Cooperation, and by Kyoto University Global COE Program "Center for Frontier Medicine".

References

- [1] International Diabetes Federation, IDF Diabetes Atlas, 5th ed., 2011.
- [2] M. Imamura, S. Maeda, Genetics of type 2 diabetes: the GWAS era and future perspectives, *Endocr. J.* 58 (2011) 723–739. (Review).
- [3] B.F. Voight, L.J. Scott, V. Steinthorsdottir, A.P. Morris, C. Dina, R.P. Welch, E. Zeggini, C. Huth, Y.S. Aulchenko, G. Thorleifsson, L.J. McCulloch, T. Ferreira, H. Grallert, N. Amin, G. Wu, C.J. Willer, S. Raychaudhuri, S.A. McCarrroll, C. Langenberg, O.M. Hofmann, J. Dupuis, L. Qi, A.V. Segrè, M. van Hoek, P. Navarro, K. Ardlie, B. Balkau, R. Benediktsson, A.J. Bennett, R. Blagieva, E. Boerwinkle, L.L. Bonnycastle, K. Bengtsson Boström, B. Bravenboer, S. Bumpstead, N.P. Burtt, G. Charpentier, P.S. Chines, M. Cornelis, D.J. Couper, G. Crawford, A.S. Doney, K.S. Elliott, A.L. Elliott, M.R. Erdos, C.S. Fox, C.S. Franklin, M. Ganser, C. Gieger, N. Grarup, T. Green, S. Griffin, C.J. Groves, C. Guiducci, S. Hadjadj, N. Hassanal, C. Herder, B. Isomaa, A.U. Jackson, P.R. Johnson, T. Jørgensen, W.H. Kao, N. Klopp, A. Kong, P. Kraft, J. Kuusisto, T. Lauritzen, M. Li, A. Lieverse, C.M. Lindgren, V. Lyssenko, M. Marre, T. Meitinger, K. Midtthjell, M.A. Morken, N. Narisu, P. Nilsson, K.R. Owen, F. Payne, J.R. Perry, A.K. Petersen, C. Platou, C. Proença, I. Prokopenko, W. Rathmann, N.W. Rayner, N.R. Robertson, G. Rocheleau, M. Roden, M.J. Sampson, R. Saxena, B.M. Shields, P. Shrader, G. Sigurdsson, T. Sparsø, K. Strassburger, H.M. Stringham, Q. Sun, A.J. Swift, B. Thorand, J. Tichet, T. Tuomi, R.M. van Dam, T.W. van Haften, T. van Herpt, J.V. van Vliet-Ostaptchouk, G.B. Walters, M.N. Weedon, C. Wijmenga, J. Wittman, R.N. Bergman, S. Cauchi, F.S. Collins, A.L. Gloyn, U. Gyllensten, T. Hansen, W.A. Hide, G.A. Hitman, A. Hofman, D.J. Hunter, K. Hveem, M. Laakso, K.L. Mohlke, A.D. Morris, C.N. Palmer, P.P. Pramstaller, I. Rudan, E. Sijbrands, L.D. Stein, J. Tuomilehto, A. Uitterlinden, M. Walker, N.J. Wareham, R.M. Watanabe, G.R. Abecasis, B.O. Boehm, H. Campbell, M.J. Daly, A.T. Hattersley, F.B. Hu, J.B. Meigs, J.S. Pankow, O. Pedersen, H.E. Wichmann, I. Barroso, J.C. Florez, T.M. Frayling, L. Groop, R. Sladek, U. Thorsteinsdottir, J.F. Wilson, T. Illig, P. Froguel, C.M. van Duijn, K. Stefansson, D. Altshuler, M. Boehnke, M.I. McCarthy, M. investigators, G. Consortium, Twelve type 2 diabetes susceptibility loci identified through large-scale association analysis, *Nat. Genet.* 42 (2010) 579–589.
- [4] K. Miyake, W. Yang, K. Hara, K. Yasuda, Y. Horikawa, H. Osawa, H. Furuta, M.C. Ng, Y. Hirota, H. Mori, K. Ido, K. Yamagata, Y. Hinokio, Y. Oka, N. Iwasaki, Y. Iwamoto, Y. Yamada, Y. Seino, H. Maegawa, A. Kashiwagi, H.Y. Wang, T. Tanahashi, N. Nakamura, J. Takeda, E. Maeda, K. Yamamoto, K. Tokunaga, R.C. Ma, W.Y. So, J.C. Chan, N. Kamatani, H. Makino, K. Nanjo, T. Kadowaki, M. Kasuga, Construction of a prediction model for type 2 diabetes mellitus in the Japanese population based on 11 genes with strong evidence of the association, *J. Hum. Genet.* 54 (2009) 236–241.
- [5] W. Bodmer, C. Bonilla, Common and rare variants in multifactorial susceptibility to common diseases, *Nat. Genet.* 40 (2008) 695–701.
- [6] W. Liu, D. Morito, S. Takashima, Y. Mineharu, H. Kobayashi, T. Hitomi, H. Hashikata, N. Matsuura, S. Yamazaki, A. Toyoda, K. Kikuta, Y. Takagi, K.H. Harada, A. Fujiyama, R. Herzig, B. Kricsek, L. Zou, J.E. Kim, M. Kitakaze, S. Miyamoto, K. Nagata, N. Hashimoto, A. Koizumi, Identification of RNF213 as a susceptibility gene for moyamoya disease and its possible role in vascular development, *PLoS One* 6 (2011) e22542.
- [7] K. Yamagata, Regulation of pancreatic beta-cell function by the HNF transcription network: lessons from maturity-onset diabetes of the young (MODY), *Endocr. J.* 50 (2003) 491–499.
- [8] T. Yorifuji, R. Fujimaru, Y. Hosokawa, N. Tamagawa, M. Shiozaki, K. Aizu, K. Jinno, Y. Maruo, H. Nagasaka, T. Tajima, K. Kobayashi, T. Urakami, Comprehensive molecular analysis of Japanese patients with pediatric-onset MODY-type diabetes mellitus, *Pediatr. Diabetes* 13 (2012) 26–32.
- [9] M.J. Bamshad, S.B. Ng, A.W. Bigham, H.K. Tabor, M.J. Emond, D.A. Nickerson, J. Shendure, Exome sequencing as a tool for Mendelian disease gene discovery, *Nat. Rev. Genet.* 12 (2011) 745–755.
- [10] C.D. Saudek, W.H. Herman, D.B. Sacks, R.M. Bergenstal, D. Edelman, M.B. Davidson, A new look at screening and diagnosing diabetes mellitus, *J. Clin. Endocrinol. Metab.* 93 (2008) 2447–2453.
- [11] S. Ellard, C. Bellanné-Chantelot, A.T. Hattersley, E.M.G.Q.N.E.M. group, Best practice guidelines for the molecular genetic diagnosis of maturity-onset diabetes of the young, *Diabetologia* 51 (2008) 546–553.
- [12] L. Kruglyak, M.J. Daly, M.P. Reeve-Daly, E.S. Lander, Parametric and nonparametric linkage analysis: a unified multipoint approach, *Am. J. Hum. Genet.* 58 (1996) 1347–1363.
- [13] Q. Zhu, K. Yamagata, A. Miura, N. Shihara, Y. Horikawa, J. Takeda, J. Miyagawa, Y. Matsuzawa, T130I mutation in HNF-4alpha gene is a loss-of-function mutation in hepatocytes and is associated with late-onset Type 2 diabetes mellitus in Japanese subjects, *Diabetologia* 46 (2003) 567–573.
- [14] A. Bonnefond, E. Durand, O. Sand, F. De Graeve, S. Gallina, K. Busiah, S. Lobbens, A. Simon, C. Bellanné-Chantelot, L. Létourneau, R. Scharfmann, J. Delplanque, R. Sladek, M. Polak, M. Vaxillaire, P. Froguel, Molecular diagnosis of neonatal diabetes mellitus using next-generation sequencing of the whole exome, *PLoS One* 5 (2010) e13630.
- [15] S. Johansson, H. Irgens, K.K. Chudasama, J. Molnes, J. Aerts, F.S. Roque, I. Jonassen, S. Levy, K. Lima, P.M. Knappskog, G.I. Bell, A. Molven, P.R. Njølstad, Exome sequencing and genetic testing for MODY, *PLoS One* 7 (2012) e38050.
- [16] A. Bonnefond, J. Philippe, E. Durand, A. Dechaume, M. Huyvaert, L. Montagne, M. Marre, B. Balkau, I. Fajardy, A. Vambergue, V. Vatin, J. Delplanque, D. Le Gulcher, F. De Graeve, C. Lecoeur, O. Sand, M. Vaxillaire, P. Froguel, Whole-exome sequencing and high throughput genotyping identified KCNJ11 as the thirteenth MODY gene, *PLoS One* 7 (2012) e37423.
- [17] D.S. Lieber, S.B. Vafai, L.C. Horton, N.G. Slate, S. Liu, M.L. Borowsky, S.E. Calvo, J.D. Schmahmann, V.K. Mootha, Atypical case of Wolfram syndrome revealed through targeted exome sequencing in a patient with suspected mitochondrial disease, *BMC Med. Genet.* 13 (2012) 3.
- [18] F.T. Mu, J.M. Callaghan, O. Steele-Mortimer, H. Stenmark, R.G. Parton, P.L. Campbell, J. McCluskey, J.P. Yeo, E.P. Toock, B.H. Toh, EEA1, an early endosome-associated protein. EEA1 is a conserved alpha-helical peripheral membrane protein flanked by cysteine "fingers" and contains a calmodulin-binding IQ motif, *J. Biol. Chem.* 270 (1995) 13503–13511.
- [19] H. Stenmark, R. Aasland, B.H. Toh, A. D'Arrigo, Endosomal localization of the autoantigen EEA1 is mediated by a zinc-binding FYVE finger, *J. Biol. Chem.* 271 (1996) 24048–24054.
- [20] A. Simonsen, R. Lippé, S. Christoforidis, J.M. Gaullier, A. Brech, J. Callaghan, B.H. Toh, C. Murphy, M. Zerial, H. Stenmark, EEA1 links PI(3)K function to Rab5 regulation of endosome fusion, *Nature* 394 (1998) 494–498.
- [21] J.J. Dumas, E. Merithew, E. Sudharshan, D. Rajamani, S. Hayes, D. Lawe, S. Corvera, D.G. Lambright, Multivalent endosome targeting by homodimeric EEA1, *Mol. Cell* 8 (2001) 947–958.
- [22] R. Cheng, J. Qiu, X.Y. Zhou, X.H. Chen, C. Zhu, D.N. Qin, J.W. Wang, Y.H. Ni, C.B. Ji, X.R. Guo, Knockdown of STEAP4 inhibits insulin-stimulated glucose transport and GLUT4 translocation via attenuated phosphorylation of Akt, independent of the effects of EEA1, *Mol. Med. Rep.* 4 (2011) 519–523.
- [23] P.A. Fujita, B. Rhead, A.S. Zweig, A.S. Hinrichs, D. Karolchik, M.S. Cline, M. Goldman, G.P. Barber, H. Clawson, A. Coelho, M. Diekhans, T.R. Dreszer, B.M. Giardine, R.A. Harte, J. Hillman-Jackson, F. Hsu, V. Kirkup, R.M. Kuhn, K. Learned,

- C.H. Li, L.R. Meyer, A. Pohl, B.J. Raney, K.R. Rosenbloom, K.E. Smith, D. Haussler, W.J. Kent, The UCSC genome browser database: update 2011, *Nucleic Acids Res.* 39 (2011) D876–D882.
- [24] E. Karakoc, C. Alkan, B.J. O’Roak, M.Y. Dennis, L. Vives, K. Mark, M.J. Rieder, D.A. Nickerson, E.E. Eichler, Detection of structural variants and indels within exome data, *Nat. Methods* 9 (2012) 176–178.
- [25] I.A. Adzhubei, S. Schmidt, L. Peshkin, V.E. Ramensky, A. Gerasimova, P. Bork, A.S. Kondrashov, S.R. Sunyaev, A method and server for predicting damaging missense mutations, *Nat. Methods* 7 (2010) 248–249.
- [26] P. Wang, B. Sun, D. Hao, X. Zhang, T. Shi, D. Ma, Human TMEM174 that is highly expressed in kidney tissue activates AP-1 and promotes cell proliferation, *Biochem. Biophys. Res. Commun.* 394 (2010) 993–999.

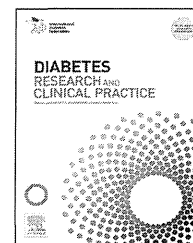


Contents available at Sciverse ScienceDirect

Diabetes Research
and Clinical Practice

journal homepage: www.elsevier.com/locate/diabres

International
Diabetes
Federation



CrossMark

A hospital-based cross-sectional study to develop an estimation formula for 2-h post-challenge plasma glucose for screening impaired glucose tolerance[☆]

Yaeko Kondo^a, Norio Harada^a, Takashi Sozu^b, Akihiro Hamasaki^a,
Shunsuke Yamane^a, Atsushi Muraoka^a, Takanari Harada^a,
Kimitaka Shibue^a, Daniela Nasteska^a, Erina Joo^a, Kazuki Sasaki^a,
Nobuya Inagaki^{a,*}

^aDepartment of Diabetes and Clinical Nutrition, Graduate School of Medicine, Kyoto University, Kyoto, Japan

^bDepartment of Biostatistics, Kyoto University School of Public Health, Kyoto, Japan

ARTICLE INFO

Article history:

Received 27 December 2012

Received in revised form

29 March 2013

Accepted 30 May 2013

Available online 24 June 2013

Keywords:

IGT

OGTT

Screening

ABSTRACT

Aims: To create and validate an estimation formula for 2-h post-challenge plasma glucose (2-hPG) as an alternative to oral glucose tolerance test (OGTT) for impaired glucose tolerance (IGT) screening.

Methods: 380 Japanese subjects (57.6% males, aged 58.5 (14.0); mean (SD) years) undergoing OGTT were included in this hospital-based cross-sectional study mainly at Kyoto University Hospital between 2000 and 2011. We determined the main predictive variables of 2-hPG from clinical variables and separated the subjects randomly into two groups: a derivation group to construct an estimation formula of 2-hPG on the basis of predictive variables and a validation group to evaluate the accuracy of the formula.

Results: Fasting plasma glucose (FPG) and hemoglobin A1c (HbA1c) were highly correlated with 2-hPG measured by OGTT. Multiple linear regression analysis showed that estimated 2-hPG (e2-hPG) was calculated by the formula: $e2\text{-hPG} = 1.66 \times \text{FPG (mmol/l)} + 1.63 \times \text{HbA1c (\%)} - 10.11$ (R^2 , coefficient of determination = 60.2%). When the cut-off value was set to the diagnostic criteria of IGT, 7.8 mmol/l of e2-hPG, sensitivity, specificity, and negative predictive value (NPV) were 83.3%, 44.1%, and 74.3%, respectively. When the cut-off value was set lower (7.2 mmol/l), these values were 94.4%, 30.5%, and 85.7%, respectively. The area under the receiver operating characteristic (ROC) curve was 0.68.

Conclusions: This high-sensitive estimation formula may be a useful alternative to OGTT for IGT screening. For the levels ≤ 7.2 mmol/l, this formula may also be useful in cross-sectional study to identify people whose glucose tolerance is normal.

© 2013 Elsevier Ireland Ltd. All rights reserved.

[☆] Presented at 'The 48th EASD (European Association for the Study of Diabetes) Annual Meeting, Berlin, Germany, 1–5 October 2012'. And also at 'The 9th IDF-WPR (International Diabetes Federation – Western Pacific Region) Congress & 4th AASD (Asian Association for the Study of Diabetes) Scientific Meeting, Kyoto, Japan, 24–27, November 2012.

* Corresponding author at: Department of Diabetes and Clinical Nutrition, Graduate School of Medicine, Kyoto University, 54 Kawaharacho, Shogoin, Sakyo-ku, Kyoto 606-8507, Japan. Tel.: +81 75 751 3562; fax: +81 75 751 6601.

E-mail address: inagaki@metab.kuhp.kyoto-u.ac.jp (N. Inagaki).

0168-8227/\$ – see front matter © 2013 Elsevier Ireland Ltd. All rights reserved.

<http://dx.doi.org/10.1016/j.diabres.2013.05.013>

1. Introduction

Impaired glucose tolerance (IGT) represents high risk not only for development of type 2 diabetes mellitus (DM) but also for cardiovascular disease [1–5]. A meta-analysis has shown that subjects with IGT have an annualized relative risk (95% confidence interval) for progression to DM of 6.35 (4.87–7.82) compared to those with normal glucose tolerance (NGT) [5]. Furthermore, it is known that lifestyle and pharmacological interventions for IGT are effective in preventing or delaying type 2 DM [6–9]. Collaborative Analysis of Diagnostic Criteria in Europe (DECOD), Collaborative Analysis of Diagnostic Criteria in Asia (DECODA), and Funagata Diabetes study have shown a strong association between postprandial hyperglycemia such as that seen in IGT and cardiovascular risk [3,10,11]. Cardiovascular mortality in subjects with IGT is similar to that in type 2 DM and much greater than that in impaired fasting glucose (IFG) [12]. Thus, detection of IGT is critical for preventing type 2 DM and reducing diabetic complications.

The “gold standard” method for diagnosing IGT defined by 1998 World Health Organization (WHO) criteria uses the level of 2-h post-challenge plasma glucose (2-hPG) during oral glucose tolerance test (OGTT) [13]. However, it is difficult to implement this test in a large population due to time and expense requirements [14]. For this reason, alternative methods for identifying IGT without OGTT have been investigated. Neither fasting plasma glucose (FPG) nor hemoglobin A1c (HbA1c) can be used singly to predict IGT due to the low detection rate [15–18]; however, combined use of FPG and HbA1c has been shown to be more effective [19]. Age, gender and body mass index (BMI) also have effects on the accuracy of IGT screening with single use of FPG and HbA1c [17,20–23]. At this point in time, there is no validated estimation formula to screen IGT that takes the predictive variables into account.

We screened for predictive variables of 2-hPG in hospital-based Japanese subjects and were able to develop an estimation formula for 2-hPG based on these predictive variables. We also validated the derived estimation formula for IGT screening which would be available for clinical settings.

2. Subjects and methods

2.1. Subjects

Three hundred eighty Japanese subjects not taking oral hypoglycemic agents and undergoing 75 g OGTT were recruited in this cross-sectional study at the Department of Diabetes and Clinical Nutrition, Kyoto University Hospital and other hospitals during the period of December 2000 through October 2011. Inclusion criteria were: family history of type 2 DM, past history of gestational diabetes, more than 20 years old, BMI > 25 kg/m², positive result of urine glucose test or hyperglycemia at examination for regular medical checkup. Exclusion criteria were: history of type 1 DM, endocrine diseases, operations such as gastrectomy and pancreatectomy, treatment with medications known to affect glucose

metabolism, and all conditions that might lead to misinterpretation of HbA1c, such as anemia. The study protocol was approved by Kyoto University Graduate School and Faculty of Medicine, Ethics Committee and conducted according to the Declaration of Helsinki. Informed consent was obtained from all subjects.

2.2. Measurements

Physical variables (age, gender, height, body weight, BMI) and laboratory variables (plasma glucose, immunoreactive insulin (IRI), HbA1c) were taken. Each standard OGTT was administered according to the National Diabetes Data Group recommendations [24]. Blood samples for determination of blood glucose levels were collected at 0, 30, 60, 90, and 120 min after oral administration of 75 g glucose. As the index of insulin secretion, we used the insulinogenic index, the change in the ratio of insulin to glucose level during the first 30 min of OGTT: $(\text{IRI } 30 \text{ min} - \text{fasting immunoreactive insulin (F-IRI)}) / (\text{PG } 30 \text{ min} - \text{FPG})$ [25,26].

2.3. Laboratory examination

PG was measured by glucose oxidase method using the Hitachi Automatic Clinical Analyzer 7170 (Hitachi, Tokyo, Japan). IRI was measured by two-site radioimmunoassay (Insulin Ria-bead II, Dainabot, Tokyo, Japan). HbA1c was measured using high performance liquid chromatography (HPLC) and is expressed as a National Glycohemoglobin Standardization Program (NGSP) equivalent value calculated by the formula: $\text{HbA1c (NGSP value) (\%)} = 1.02 \times \text{HbA1c (Japan Diabetes Society value) (\%)} + 0.25$ [27]. The HbA1c measurements in International Federation of Clinical Chemistry (IFCC) units (mmol/mol) were also calculated.

2.4. Definitions

According to the 1998 WHO diagnostic criteria [13], the subjects were classified into the following four subgroups: NGT; $\text{FPG mmol/l} < 6.1 \text{ mmol/l}$ and $\text{2-hPG} < 7.8 \text{ mmol/l}$, IGT; $\text{FPG} < 7.0 \text{ mmol/l}$ and $7.8 \text{ mmol/l} \leq \text{2-hPG} < 11.1 \text{ mmol/l}$, IFG; $6.1 \text{ mmol/l} \leq \text{FPG} < 7.0 \text{ mmol/l}$ and $\text{2-hPG} < 7.8 \text{ mmol/l}$, DM: $7.0 \text{ mmol/l} \leq \text{FPG}$ or $11.1 \text{ mmol/l} \leq \text{2-hPG}$.

As shown in the supplemental table, sensitivity was defined as the proportion of subjects with IGT by OGTT who were predicted to have a positive result by the estimation formula: $\{a/(a+c)\} \times 100$ (%). Specificity was defined as the proportion of subjects without IGT who were predicted not to have IGT; $\{d/(b+d)\} \times 100$ (%). Positive predictive value (PPV) was defined as the proportion of subjects predicted to have IGT who were truly IGT by OGTT; $\{a/(a+b)\} \times 100$ (%). Negative predictive value (NPV) was defined as the proportion of subjects predicted not to have IGT who were truly not IGT by OGTT; $\{d/(c+d)\} \times 100$ (%). A receiver operating characteristic (ROC) curve was constructed by plotting sensitivity against the false-positive rate (100 – specificity) (%) over a range of cut-off values.

Supplementary material related to this article found, in the online version, at <http://dx.doi.org/10.1016/j.diabres.2013.05.013>.

2.5. Statistical analyses

Statistical analyses were performed according to the following steps.

- (1) Background of the subjects: results were expressed as mean (standard deviation: SD or mean standard error: SE). Differences between the two groups were compared using the Student's t-test. *P* value < .05 (two-tailed) was considered as statistically significant.
- (2) The relationship between two variables: the relationship between measured 2-h post-challenge plasma glucose (m2-hPG) and clinical variables was evaluated by scatter plot and Pearson's correlation coefficient (*r*).
- (3) Derivation and validation: to avoid over-fitting of the estimation formula, two-step procedure was used. A total of 380 subjects were randomly divided into two groups at 1 to 1 ratio, a derivation group for constructing the estimation formula to screen IGT and a validation group without DM for evaluating the accuracy of the derived estimation formula.
- (4) Construction of the estimation formula in the derivation group: higher values of correlation coefficient demonstrated in the previous step were regarded as predictive

variables for m2-hPG, and the estimation formula of 2-hPG with these variables was then constructed by multiple linear regression analysis.

- (5) Evaluation of the derived estimation formula in the validation group: the diagnostic characteristics such as sensitivity, specificity, PPV, and NPV of this derived estimation formula were calculated. The performance of the estimation formula was assessed by calculating the area under the ROC curve based on sensitivity and specificity [28]. In addition, we determined the adequate cut-off value by considering these values.

All statistical analyses were performed using SAS version 9.2 (SAS Institute Inc, Cary, NC).

3. Results

3.1. Characteristics of the subjects

Clinical characteristics of the subjects are shown in Table 1. Results of age and HbA1c are shown as mean (SD); the others are shown as mean (SE). Because the number of IFG (*n* = 9) was too small for analysis, we compared physical and metabolic

Table 1 – Characteristics of the subjects.

	NGT	IFG	IGT	DM	Total
Number (%)	126 (33.2)	9 (2.4)	106 (27.9)	139 (36.6)	380 (100)
Male (%)	60 (47.6)	6 (66.7)	50 (47.2)	103 (74.1)	219 (57.6)
Age (year) [†]	54.5 (15.5)	61.4 (15.5)	57.0 (13.3)	63.2 (11.6)	58.5 (14.0)
BMI (kg/m ²) [‡]	23.5 (4.8)	26.1 (2.4)	25.9 (5.6)	24.4 (3.5)	24.6 (4.7)
			**vs. NGT		
			vs. DM		
HbA1c (%) [†]	5.9 (0.6)	6.5 (0.6)	6.2 (0.5)	7.0 (0.6)	6.4 (0.7)
			***vs. NGT	***vs. NGT	
				***vs. IGT	
HbA1c (mmol/mol)	40.9 (6.1)	47.5 (6.3)	44.0 (5.2)	53.1 (6.5)	46.0 (8.0)
			***vs. NGT	***vs. NGT	
				***vs. IGT	
F-IRI (pmol/l) [†]	36.0 (24.8)	50.7 (32.6)	43.7 (28.1)	41.7 (25.0)	40.6 (26.2)
			vs. NGT	vs. NGT	
2-hIRI (pmol/l) [†]	222.3 (155.6)	354.7 (282.4)	351.9 (217.9)	274.2 (180.5)	282.7 (194.6)
			***vs. NGT	vs. NGT	
				vs. IGT	
FPG (mmol/l) [†]	5.1 (0.5)	6.5 (0.2)	5.5 (0.6)	7.0 (1.2)	6.0 (1.2)
			***vs. NGT	***vs. NGT	
				***vs. IGT	
2-hPG (mmol/l) [†]	6.2 (1.1)	6.8 (0.7)	9.4 (0.9)	14.6 (2.8)	10.2 (4.0)
			***vs. NGT	***vs. NGT	
				***vs. IGT	
Insulinogenic index [†]	65.1 (38.4)	31.2 (24.2)	38.5 (24.6)	15.8 (6.5)	33.8 (17.9)
			***vs. NGT	***vs. NGT	
				***vs. IGT	

Abbreviations: BMI, body mass index; HbA1c, hemoglobin A1c; F-IRI, fasting immunoreactive insulin; 2-hIRI, 2-h immunoreactive insulin; FPG, fasting plasma glucose; 2-hPG, 2-h post-challenge plasma glucose; NGT, normal glucose tolerance; IFG, impaired fasting glucose; IGT, impaired glucose tolerance; DM, diabetes mellitus; SD, standard deviation; SE, standard error.

* *P* < .05.

** *P* < .01.

*** *P* < .001.

[†] Data are described means (SD).

[‡] Data are described means (SE).

variables among the three other groups (NGT, IGT, and DM). The total of mean age (SD) is 58.5 (14.0) years and 57.6% are males. Age of DM subjects is the highest ($P < .01$ vs. NGT) and BMI of IGT subjects is the highest ($P < .01$ vs. NGT and $P < .05$ vs. DM, respectively) among the three groups. HbA1c is significantly higher, while insulinogenic index is significantly lower in subjects with DM than in those with NGT and IGT. Glucose and plasma insulin levels during OGTT are given in the supplemental figure. For plasma glucose, subjects with NGT are those with 5.1 (0.5) mmol/l of FPG and 6.2 (1.1) mmol/l of 2-hPG (Supplemental Figure A). For subjects with IFG, FPG is 6.5 (0.2) mmol/l and for those with IGT, 2-hPG is 9.4 (0.9) mmol/l. For subjects with DM, FPG is 7.0 (1.2) mmol/l and 2-hPG is 14.6 (2.8) mmol/l. Early-phase insulin secretion shown in Supplemental Figure B is already decreased in the IGT stage as shown in the previous Japanese study [29].

Supplementary material related to this article found, in the online version, at <http://dx.doi.org/10.1016/j.diabres.2013.05.013>.

3.2. Relationship between two variables

We evaluated the relationship among all pairs of continuous variables using scatter plot and calculated Pearson's correlation coefficient. Using this procedure, we found the predictive variables for m2-hPG in this target population.

Fig. 1 shows the scatter plot of m2-hPG and FPG (Fig. 1A) and that of m2-hPG and HbA1c (Fig. 1B) in OGTT of all subjects. The correlation coefficient (r) between two variables is 0.74 and 0.67, respectively. Except for these two variables, there is no higher correlation coefficient than 0.5 between m2-hPG and the physical, metabolic variables.

3.3. Construction of the estimation formula in the derivation group

First, all subjects were randomly divided 1:1 into the derivation group and the validation group to avoid over-fitting.

At a stage prior to this, FPG and HbA1c were substantiated as main predictive variables for m2-hPG, then the estimation formula with these variables was constructed by using the multiple linear regression analysis in the derivation group. The obtained linear regression equation (estimation formula) is $e2\text{-hPG} = 1.66 \times \text{FPG (mmol/l)} + 1.63 \times \text{HbA1c (NGSP: \%)} - 10.11$, or $e2\text{-hPG} = 1.66 \times \text{FPG (mmol/l)} + 0.15 \times \text{HbA1c (mmol/mol)} - 6.61$. R^2 (coefficient of determination) is 60.2%. Moreover, we analyzed to determine whether inclusion of other variables known to affect 2-hPG improved the accuracy of this formula. Even though other variables such as BMI, age, gender, and IRI are included in the regression model, R^2 remains substantially unchanged (data not shown). FPG and HbA1c are thus the best predictors of 2-hPG based on the linear regression model and we concluded the estimation formula of 2-hPG shown in Fig. 2 in this derivation group.

3.4. Evaluation of the derived estimation formula in the validation group

The accuracy of this estimation formula: diagnostic characteristics such as sensitivity, specificity, PPV, NPV, and the area under the ROC curve were calculated in the validation group. Table 2 shows the results of sensitivity, specificity, PPV, and NPV for every 0.2 mmol/l of e2-hPG in this group. When the cut-off value is set to the diagnostic criteria of IGT, 7.8 mmol/l of e2-hPG, sensitivity, specificity and NPV of this formula are 83.3%, 44.1%, and 74.3%, respectively. When the cut-off value is ≤ 7.8 mmol/l of e2-hPG, sensitivity is retained more than 80%, and when lowered to 7.2 mmol/l of e2-hPG, sensitivity, specificity, and NPV are 94.4%, 30.5% and 85.7%, respectively. These results are plotted in Fig. 3. In the validation group, the ROC curves obtained by calculating sensitivity and specificity at possible cut-off points of estimated 2-hPG are also shown in Fig. 3. The performance of the estimation formula was assessed by calculating the area under the ROC curve, which is 0.68.

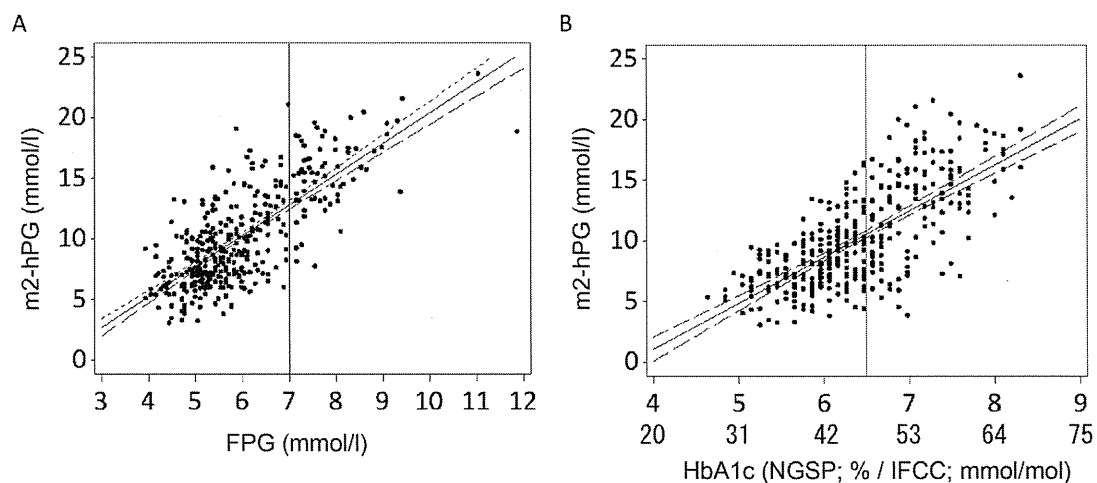


Fig. 1 – Scatter plot of measured 2-hPG (m2-hPG) and FPG in OGTT (A) and that of m2-hPG and HbA1c in OGTT (B); the correlation coefficient (r) = 0.74, 0.67, respectively.

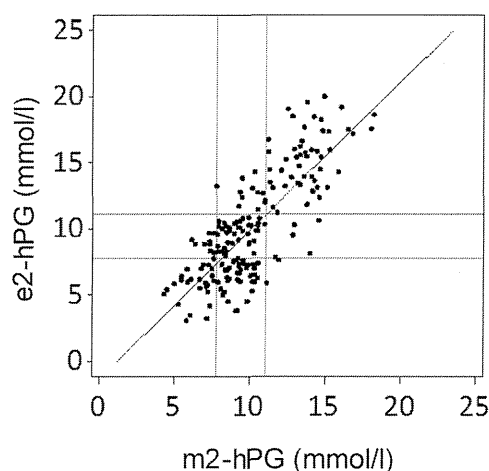


Fig. 2 – Scatter plot and the estimation formula of estimated 2h-PG (e2-hPG) in derivation group. $e2\text{-hPG} = 1.66 \times \text{FPG (mmol/l)} + 1.63 \times \text{HbA1c (\%)} - 10.11$ ($R^2 = 60.2\%$). $e2\text{-hPG} = 1.66 \times \text{FPG (mmol/l)} + 0.15 \times \text{HbA1c (mmol/mol)} - 6.61$ ($R^2 = 60.2\%$).

4. Discussion

In the present study, we found that the main predictive variables associated with m2-hPG are FPG and HbA1c from the data of 380 hospital-based Japanese subjects. We were able to develop a validated estimation formula for 2-hPG with these variables as an alternative to OGTT for IGT screening.

Studies have reported that lifestyle and pharmacological intervention for subjects with IGT can prevent or delay the onset of type 2 DM [6–9]. Detection and early intervention for these high-risk individuals is critical for preventing type 2 DM and reducing diabetic complications. Even though OGTT is the “gold standard” method for diagnosing IGT, in a large population that method is time-consuming and expensive [14].

Some studies have investigated alternative methods for evaluating IGT without performing OGTT [15–23]. The single

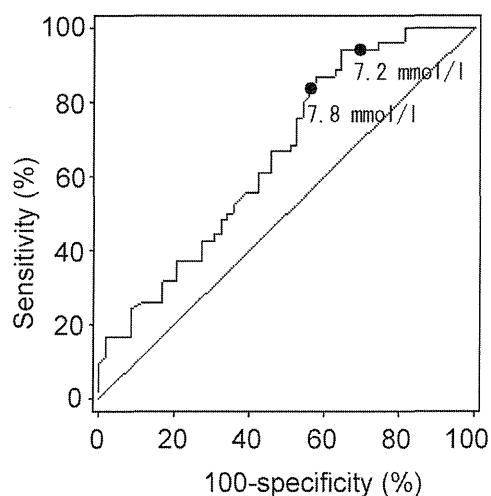


Fig. 3 – Receiver operating characteristic (ROC) curves obtained by calculating sensitivity and specificity at possible cut-off points of estimated 2-hPG in validation group. The horizontal axis shows the (100 – specificity) (%) and the vertical axis shows the sensitivity (%). When the cut-off value is set to the diagnostic criteria of IGT, 7.8 mmol/l of e2-hPG, sensitivity and specificity are 83.3% and 44.1%, respectively. When the cut-off value is set lowered to 7.2 mmol/l of e2-hPG, those are 94.4% and 30.5%, respectively. The area under the ROC curve is 0.68.

use of FPG or HbA1c is not suitable for IGT screening because of the low detection rate [15–18]. It was reported in a systematic review that for detecting IGT by HbA1c or FPG separately, that sensitivity is around 50% [16]. Indeed, in our result, with single use of FPG or HbA1c, R^2 was 56.2% and 48.3%, respectively (Fig. 1), while using the estimation formula with both FPG and HbA1c, R^2 was 60.2% (Fig. 2) for IGT screening. This result is compatible with the previous study recommending the combined use of these two variables to be more effective than single use for detecting IGT [19]. But this study did not elucidate the influence of each of the variables on 2-hPG.

Table 2 – Summary of sensitivity, specificity, PPV, and NPV for every 0.2 mmol/l of estimated 2-hPG (e-2hPG) in the validation group.

Cut-off value of e2-hPG (mmol/l)	Sensitivity (%)	Specificity (%)	PPV (%)	NPV (%)
6.8	96.3	23.7	53.6	87.5
7.0	96.3	25.4	54.2	88.2
7.2	94.4	30.5	55.4	85.7
7.4	87.0	37.3	56.0	75.9
7.6	87.0	40.7	57.3	77.4
7.8	83.3	44.1	57.7	74.3
8.0	70.4	47.5	55.1	63.6
8.2	66.7	52.5	56.3	63.3
8.4	61.1	57.6	56.9	61.8
8.6	53.7	62.7	56.9	59.7
8.8	50.0	66.1	57.4	59.1

PPV, positive predictive value; NPV, negative predictive value.

Caucasians generally have higher BMI and insulin resistance is important in progression from NGT to IGT [30], while Asians including Japanese are generally less obese and have higher insulin sensitivity than Caucasians. Several previous studies reported that BMI is a helpful factor for IGT screening [17,20–23]. High BMI (>27 or >30 kg/m²) is associated with higher prevalence of IGT compared to that with BMI <25 kg/m². Hiltunen et al. reported that higher BMI (>30 kg/m²) was the best predictor of IGT in a Finland population-based study and Saydah SH et al. reported that BMI (>30 kg/m²) and age in addition to FPG or HbA1c can be used to improve the sensitivity for detecting IGT without OGTT among U.S. populations [20,23]. Contrary to these reports, we did not find a high correlation between 2-hPG and BMI ($r = 0.03$). The proportion of obesity of these studies is high, the ratio of BMI >27 kg/m² and >30 kg/m² are 53% and 24%, respectively [20,23], while in our study the mean (SD) of BMI was 24.6 (4.7) kg/m² and the ratio of obese subjects with BMI >30 kg/m² are only 1%. It was reported previously that the difference with or without the obesity (BMI >25 kg/m²) did not contribute to IGT screening in Japanese [21]. The BMI used in the study was similar to that in our study (BMI: 23–25 kg/m²). On the other hand, insulin secretion rather than insulin resistance is a more significant factor in progression from NGT to type 2 DM via IGT in Asian diabetes [29,31–35]. Indeed, in the present study insulin secretion is decreased gradually from NGT via IGT to type 2 DM (65.1, 38.5, 15.8, respectively) as in other previous reports in Asian diabetes [31,35] (Table 1). Taken together, the discrepancy of the correlation may be due to the ethnic differences such as BMI and insulin secretory capacity. The variables affecting 2-hPG during OGTT might differ among ethnic populations and require a different estimation formula and adequate cut-off value to identify IGT. It is also reported that age has an effect on the accuracy of IGT screening [22]. In our study, however, there was low correlation between 2-hPG and age ($r = 0.24$). The reason may be the different methods of analysis. We considered age from 20 to 89 years as a continuous variable rather than as a categorical one with relatively narrow age. In addition, gender was not an independent predictive variable for 2-hPG and even though included in the regression model, R² remains substantially unchanged in our study (data not shown).

Generally, the performance of a screening test depends on the cut-off value and it is rare to have both high sensitivity and specificity. The priority in this trade-off is determined by the characteristics of the condition to be diagnosed [36,37]. In the case of IGT, mis-identifying IGT subjects as normal (false negatives) is more critical than classifying healthy subjects as abnormal (false positives), since these subjects are at high risk for cardiovascular diseases as well as diabetes and its complications. Thus, a screening test for IGT should prioritize high sensitivity to decrease the false-negatives. As summarized in Table 2, when the cut-off value was set to the diagnostic criteria of IGT, 7.8 mmol/l of e2-hPG, sensitivity of this formula was 83.3%. However, even with this cut-off value, NPV still remained 74.3%. If the cut-off value was lowered to 7.2 mmol/l, NPV was up to 85.7% with 94.4% sensitivity. When a screening test has high sensitivity, subjects having a negative result can be judged as negative with high precision

[36–39]. The rule of SnNout states that if a screening test has high sensitivity (Sn), a negative result (N) rules out (Out) the target disorder, which describes IGT in our study. In accord with this theory, using our high-sensitive estimation formula for IGT screening and with the cut-off value set to 7.2 mmol/l of e2-hPG with 94.4% sensitivity, the subjects with e2-hPG ≤ 7.2 mmol/l were ruled out of the diagnosis of IGT. Thus, further OGTT to diagnose whether or not they have IGT may not be necessary for these low risk subjects.

Our study has several limitations. One is the high prevalence of type 2 DM subjects in our hospital-based study. It is reported that the prevalence of type 2 DM varies across studies, in hospital-based studies ranging from 10 to 44% and in community-based studies ranging from 6.2 to 7.4% [16]. While the proportion of subgroups in OGTT would affect the efficacy of the estimation formula, there are at present no established data of general population-based or hospital-based studies. Thus, no comparisons are possible between our results with previous findings. Another limitation is screening bias because it is a cross-sectional study. There are no definite inclusion criteria—they depend on the individual judgment of each doctor. Our results regarding sensitivity, specificity, and cut-off value are internally validated, but it remains to be determined whether these findings apply to other populations: generation-based or higher BMI like Caucasian and so on. Therefore further studies are required to validate in the broader population.

In conclusion, our high-sensitivity estimation formula based on FPG and HbA1c may be useful in screening for IGT. More than 80% sensitivity of this formula was preserved at ≤ 7.8 mmol/l of e2-hPG in this hospital-based study. In addition, when the levels of e2-hPG are ≤ 7.2 mmol/l, this estimation formula can be used to identify subjects with normal glucose tolerance.

Conflict of interest

The authors declare that they have no conflict of interest.

Acknowledgement

This study was supported by Scientific Research Grants from the Ministry of Education, Culture, Sports, Science, and Technology of Japan.

REFERENCES

- [1] Blake DR, Meigs JB, Muller DC, Najjar SS, Andres R, Nathan DM. Impaired glucose tolerance, but not impaired fasting glucose, is associated with increased levels of coronary heart disease risk factors: results from the Baltimore Longitudinal Study on Aging. *Diabetes* 2004;53(8): 2095–100.
- [2] Rodriguez BL, Curb JD, Burchfiel CM, Huang B, Sharp DS, Lu GY, et al. Impaired glucose tolerance, diabetes, and cardiovascular disease risk factor profiles in the elderly, the Honolulu Heart Program. *Diabetes Care* 1996;19(6): 587–90.

- [3] Tominaga M, Eguchi H, Manaka H, Igarashi K, Kato T, Sekikawa A. Impaired glucose tolerance is a risk factor for cardiovascular disease, but not impaired fasting glucose: the Funagata diabetes study. *Diabetes Care* 1999;22(6): 920–4.
- [4] Fuller JH, Shipley MJ, Rose G, Jarrett RJ, Keen H. Coronary-heart-disease risk and impaired glucose tolerance: the Whitehall study. *Lancet* 1980;1(8183):1373–6.
- [5] Gerstein HC, Santaguida P, Raina P, Morrison KM, Balion C, Hunt D, et al. Annual incidence and relative risk of diabetes in people with various categories of dysglycemia: a systematic overview and meta-analysis of prospective studies. *Diabetes Res Clin Pract* 2007;78(3):305–12.
- [6] Knowler WC, Barrett-Connor E, Fowler SE, Hamman RF, Lachin JM, Walker EA, et al. Reduction in the incidence of type 2 diabetes with lifestyle intervention or metformin. *N Engl J Med* 2002;346(6):393–403.
- [7] Tuomilehto J, Lindström J, Eriksson JG, Valle TT, Hämäläinen H, Ilanne-Parikka P, et al. Prevention of type 2 diabetes mellitus by changes in lifestyle among subjects with impaired glucose tolerance. *N Engl J Med* 2001;344(18):1343–50.
- [8] Chiasson JL, Josse RG, Gomis R, Hanefeld M, Karasik A, Laakso M. Acarbose for prevention of type 2 diabetes mellitus: the STOP-NIDDM randomised trial. *Lancet* 2002;359(9323):2072–7.
- [9] Gillies CL, Abrams KR, Lambert PC, Cooper NJ, Sutton AJ, Hsu RT, et al. Pharmacological and lifestyle interventions to prevent or delay type 2 diabetes in people with impaired glucose tolerance: systematic review and meta-analysis. *BMJ* 2007;334(7588):299.
- [10] DECODE Study Group, the European Diabetes Epidemiology Group. Glucose tolerance and cardiovascular mortality: comparison of fasting and 2-hour diagnostic criteria. *Arch Intern Med* 2001;161(3):397–405.
- [11] Nakagami T, DECODA Study Group. Hyperglycaemia and mortality from all causes and from cardiovascular disease in five populations of Asian origin. *Diabetologia* 2004;47(3):358–94.
- [12] DeFronzo RA, Abdul-Ghani M. Assessment and treatment of cardiovascular risk in prediabetes: impaired glucose tolerance and impaired fasting glucose. *Am J Cardiol* 2011;108(Suppl. 3):3B–24B.
- [13] Alberti KG, Zimmet PZ. Definition, diagnosis and classification of diabetes mellitus and its complications. Part 1. Diagnosis and classification of diabetes mellitus provisional report of a WHO consultation. *Diabet Med* 1998;15(7):539–53.
- [14] Report of the Expert Committee on the diagnosis and classification of diabetes mellitus. *Diabetes Care* 1997;20(7):1183–97.
- [15] Pinelli NR, Jantz AS, Martin ET, Jaber LA. Sensitivity and specificity of glycated hemoglobin as a diagnostic test for diabetes and prediabetes in Arabs. *J Clin Endocrinol Metab* 2011;96(10):E1680–3.
- [16] Bennett CM, Guo M, Dharmage SC. HbA(1c) as a screening tool for detection of type 2 diabetes: a systematic review. *Diabet Med* 2007;24(4):333–43.
- [17] Mannucci E, Bardini G, Ognibene A, Rotella CM. Comparison of ADA and WHO screening methods for diabetes mellitus in obese patients. *American Diabetes Association. Diabet Med* 1999;16(7):579–85.
- [18] Motala AA, Omar MA. The value of glycosylated haemoglobin as a substitute for the oral glucose tolerance test in the detection of impaired glucose tolerance (IGT). *Diabetes Res Clin Pract* 1992;17(3):199–207.
- [19] Hu Y, Liu W, Chen Y, Zhang M, Wang L, Zhou H, et al. Combined use of fasting plasma glucose and glycated hemoglobin A1c in the screening of diabetes and impaired glucose tolerance. *Acta Diabetol* 2010;47(3): 231–6.
- [20] Saydah SH, Byrd-Holt D, Harris MI. Projected impact of implementing the results of the diabetes prevention program in the U.S. population. *Diabetes Care* 2002;25(11):1940–5.
- [21] Gomyo M, Sakane N, Kamae I, Sato S, Suzuki K, Tominaga M, et al. Effects of sex, age and BMI on screening tests for impaired glucose tolerance. *Diabetes Res Clin Pract* 2004;64(2):129–36.
- [22] Nelson KM, Boyko EJ. Third National Health and Nutrition Examination Survey, Predicting impaired glucose tolerance using common clinical information: data from the Third National Health and Nutrition Examination Survey. *Diabetes Care* 2003;26(7):2058–62.
- [23] Hiltunen L, Kivelä SL, Läärä E, Keinänen-Kiukaanniemi S. Progression of normal glucose tolerance to impaired glucose tolerance or diabetes in the elderly. *Diabetes Res Clin Pract* 1997;35(2–3):99–106.
- [24] Classification and diagnosis of diabetes mellitus and other categories of glucose intolerance. National Diabetes Data Group. *Diabetes* 1979;28(12):1039–57.
- [25] Seltzer HS, Allen EW, Herron Jr AL, Brennan MT. Insulin secretion in response to glycemic stimulus: relation of delayed initial release to carbohydrate intolerance in mild diabetes mellitus. *J Clin Invest* 1967;46(3): 323–35.
- [26] Seino Y, Ikeda M, Yawata M, Imura H. The insulinogenic index in secondary diabetes. *Horm Metab Res* 1975;7(2): 107–15.
- [27] Kashiwagi A, Kasuga M, Araki E, Oka Y, Hanafusa T, Ito H, et al. International clinical harmonization of glycated hemoglobin in Japan: from Japan Diabetes Society to National Glycohemoglobin Standardization Program values. *J Diabetes Invest* 2012;3(1):39–40.
- [28] Hanley JA, McNeil BJ. The meaning and use of the area under a receiver operating characteristic (ROC) curve. *Radiology* 1982;143(1):29–36.
- [29] Fukushima M, Suzuki H, Seino Y. Insulin secretion capacity in the development from normal glucose tolerance to type 2 diabetes. *Diabetes Res Clin Pract* 2004;66(Suppl. 1): S37–43.
- [30] Saad MF, Knowler WC, Pettitt D, Nelson RG, Charles MA, Bennet P. A two-step model for development of non-insulin-dependent diabetes. *Am J Med* 1991;90: 229–35.
- [31] Suzuki H, Fukushima M, Usami M, Ikeda M, Taniguchi A, Nakai Y, et al. Factors responsible for development from normal glucose tolerance to isolated postchallenge hyperglycemia. *Diabetes Care* 2003;26(4): 1211–5.
- [32] Haffner SM, Howard G, Mayer E, Bergman RN, Savage PJ, Rewers M, et al. Insulin sensitivity and acute insulin response in African-Americans, non-Hispanic whites, and Hispanics with NIDDM: the Insulin Resistance Atherosclerosis Study. *Diabetes* 1997;46(1):63–9.
- [33] Matsumoto K, Miyake S, Yano M, Ueki Y, Yamaguchi Y, Akazawa S, et al. Glucose tolerance, insulin secretion, and insulin sensitivity in nonobese and obese Japanese subjects. *Diabetes Care* 1997;20(10):1562–8.
- [34] Mitrakou A, Kelley D, Mokan M, Veneman T, Pangburn T, Reilly J, et al. Role of reduced suppression of glucose production and diminished early insulin release in impaired glucose tolerance. *N Engl J Med* 1992;326(1): 22–9.
- [35] Fukushima M, Usami M, Ikeda M, Nakai Y, Taniguchi A, Matsuura T, et al. Insulin secretion and insulin sensitivity at different stages of glucose tolerance: a cross-sectional

- study of Japanese type 2 diabetes. *Metabolism* 2004;53(7):831-5.
- [36] Fletcher RH, Fletcher SW, Wagner EH. *Clinical epidemiology. The essentials*, 3rd ed., Baltimore: Williams and Wilkins; 1996.
- [37] Hennekens CH, Buring JE, Mayrent SL. *Epidemiology in medicine*. Boston: Little Brown; 1987.
- [38] Sackett DL, Straus SE, Richardson WS, Rosenberg W, Haynes RB. *Evidence-based medicine. How to practice and teach EBM*. New York: Churchill Livingstone; 2000.
- [39] Sackett DL, Haynes RB, Guyatt GH, Tugwell P. *Clinical epidemiology, a basic science for clinical medicine*. Boston: Little Brown; 1992.

Tetrahydrobiopterin Has a Glucose-Lowering Effect by Suppressing Hepatic Gluconeogenesis in an Endothelial Nitric Oxide Synthase–Dependent Manner in Diabetic Mice

Abulizi Abudukadier,¹ Yoshihito Fujita,¹ Akio Obara,¹ Akiko Ohashi,² Toru Fukushima,¹ Yuichi Sato,¹ Masahito Ogura,¹ Yasuhiko Nakamura,¹ Shimpei Fujimoto,¹ Masaya Hosokawa,¹ Hiroyuki Hasegawa,² and Nobuya Inagaki¹

Endothelial nitric oxide synthase (eNOS) dysfunction induces insulin resistance and glucose intolerance. Tetrahydrobiopterin (BH₄) is an essential cofactor of eNOS that regulates eNOS activity. In the diabetic state, BH₄ is oxidized to 7,8-dihydrobiopterin, which leads to eNOS dysfunction owing to eNOS uncoupling. The current study investigates the effects of BH₄ on glucose metabolism and insulin sensitivity in diabetic mice. Single administration of BH₄ lowered fasting blood glucose levels in wild-type mice with streptozotocin (STZ)-induced diabetes and alleviated eNOS dysfunction by increasing eNOS dimerization in the liver of these mice. Liver has a critical role in glucose-lowering effects of BH₄ through suppression of hepatic gluconeogenesis. BH₄ activated AMP kinase (AMPK), and the suppressing effect of BH₄ on gluconeogenesis was AMPK-dependent. In addition, the glucose-lowering effect and activation of AMPK by BH₄ did not appear in mice with STZ-induced diabetes lacking eNOS. Consecutive administration of BH₄ in *ob/ob* mice ameliorated glucose intolerance and insulin resistance. Taken together, BH₄ suppresses hepatic gluconeogenesis in an eNOS-dependent manner, and BH₄ has a glucose-lowering effect as well as an insulin-sensitizing effect in diabetic mice. BH₄ has potential in the treatment of type 2 diabetes. *Diabetes* 62:3033–3043, 2013

Nitric oxide (NO) is a biological messenger produced by NO synthase (NOS), which includes endothelial (eNOS), inducible (iNOS), and neuronal (nNOS) isoforms. eNOS-derived NO is well-known to have a pivotal role in physiological regulation of endothelial function (1,2). eNOS dysfunction occurs in conditions of diabetes and is known to induce insulin resistance and glucose intolerance (3–5). Insulin resistance caused by eNOS dysfunction is thought to be induced by endothelial dysfunction, leading to decreased skeletal muscle blood flow and glucose uptake (4). On the other hand, glucose transport in isolated skeletal muscle is lower in eNOS-deficient (eNOS^{-/-}) mice, indicating that eNOS expressed in skeletal muscle also regulates its glucose

uptake (4). Moreover, eNOS^{-/-} mice are insulin resistant at the level of liver (5). These studies suggest that eNOS plays a central role in the regulation of glucose metabolism and insulin sensitivity and represents several therapeutic targets for type 2 diabetes.

The function of eNOS is regulated by multiple factors such as mRNA expression of eNOS, L-arginine, influx of Ca²⁺, and tetrahydrobiopterin (BH₄) (2,6,7). BH₄ is an essential cofactor for eNOS catalysis and functions as an allosteric modulator of arginine binding (7,8). Binding of BH₄ to eNOS elicits a conformational change that increases the affinity for binding of arginine-based ligands. BH₄ binding also plays a role in dimer formation of the active and stabilized form of eNOS (8). BH₄ is converted to 7,8-dihydrobiopterin (BH₂) by exposure to oxidative stress such as diabetes (8,9). Increase in BH₂ induces dysfunction of eNOS, as BH₂ is inactive for NOS cofactor function and competes with BH₄ for BH₄ binding (8,9). Furthermore, in states of diabetes and high glucose, de novo synthesis of BH₄, which is rate limited by GTP cyclohydrolase I (GTPCH I), is impaired (10–13). Thus, the availability of BH₄ is reduced and the function of eNOS is altered so that the enzyme produces superoxide anion (O₂⁻) rather than NO, a phenomenon called “eNOS uncoupling” (7,8,14). Supplementation of BH₄ can improve endothelial dysfunction by elevating the BH₄-to-BH₂ ratio, leading to recoupling of eNOS, and has been used in clinical trials with patients with atherosclerotic diseases for the expected vasodilatation effects of BH₄ through NO production (15). However, it is unclear whether BH₄ improves glucose metabolism and insulin sensitivity in diabetic conditions.

In the current study, we investigated the effects of BH₄ on blood glucose levels and insulin sensitivity in diabetic mice. Fasting blood glucose levels are regulated by the level of hepatic gluconeogenesis, elevation of which is the major cause of fasting hyperglycemia in diabetes (16,17). We demonstrate here that BH₄ lowers fasting blood glucose levels and suppresses gluconeogenesis in liver in an eNOS-dependent manner. In addition, BH₄ has an ameliorating effect on glucose intolerance as well as insulin resistance in diabetic mice. Using primary hepatocytes isolated from mouse liver, we have clarified the mechanism by which BH₄ suppresses hepatic gluconeogenesis. These data suggest that BH₄ has potential as a novel therapeutic approach to diabetes.

RESEARCH DESIGN AND METHODS

Male C57/BL6 (wild-type) mice and male heterozygous *Ins2^{Akita}* (diabetic Akita) mice, which exhibit hyperglycemia with reduced β -cell mass caused by a point

From the ¹Department of Diabetes and Clinical Nutrition, Graduate School of Medicine, Kyoto University, Kyoto, Japan; and the ²Department of Functional Morphology, Nihon University School of Medicine, Tokyo, Japan. Corresponding author: Nobuya Inagaki, inagaki@metab.kuhp.kyoto-u.ac.jp. Received 10 September 2012 and accepted 27 April 2013. DOI: 10.2337/db12-1242

This article contains Supplementary Data online at <http://diabetes.diabetesjournals.org/lookup/suppl/doi:10.2337/db12-1242/-/DC1>.

© 2013 by the American Diabetes Association. Readers may use this article as long as the work is properly cited, the use is educational and not for profit, and the work is not altered. See <http://creativecommons.org/licenses/by-nc-nd/3.0/> for details.

mutation in the insulin 2 gene that leads to misfolded insulin and severe endoplasmic reticulum stress, were obtained from Shimizu (Kyoto, Japan) (18). Male eNOS^{-/-} mice in the C57/BL6 mice background were obtained from The Jackson Laboratory (Bar Harbor, ME). Male B6.V-Lepob/J (*ob/ob*) mice were obtained from Charles River Japan (Yokohama, Japan). Mice with streptozotocin (STZ)-induced diabetes were made by injection of STZ (120 mg/kg i.p.) to 7-week-old wild-type or eNOS^{-/-} mice. At 3 weeks after injection of STZ, the animals were confirmed to be diabetic by both high blood glucose levels (≥ 15 mmol/L) and other diabetic features, including polyuria, polydipsia, and hyperglycemia.

The mice were maintained in a temperature-controlled (25 \pm 2°C) environment with a 12-h light/dark cycle with free access to standard laboratory chow and water. All experiments were carried out with mice aged 8–10 weeks. The animals were maintained and used in accordance with the Guidelines for Animal Experiments of Kyoto University. All experiments involving animals were conducted in accordance with the Guidelines for Animal Experiments of Kyoto University and were approved by the Animal Research Committee, Graduate School of Medicine, Kyoto University.

Preparations and cultures of mouse hepatocyte and aortic endothelial cell. Mouse hepatocytes were isolated by collagenase digestion as previously described (19). Primary hepatocytes were prepared by seeding in sixwell type 1 collagen-coated plates at a density of 1.5×10^6 cells in Dulbecco's modified Eagle's medium (DMEM) (low glucose, 5.6 mmol/L) containing 10% (vol/vol) FBS, 100 nmol/L regular insulin, 50 units/mL penicillin, and 50 μ g/mL streptomycin. Hepatocytes were then cultured overnight in a humidified atmosphere (5% CO₂) at 37°C. As for mouse endothelial cells (ECs), the aorta was dissected and filled with collagenase type II solution. After incubation for 45 min at 37°C, ECs were removed from the aorta and collected by centrifugation at 1,200 rpm for 5 min. The EC was cultured in a sixwell collagen type I-coated dish for 1 week. **Glucose production via gluconeogenesis in hepatocytes.** Freshly isolated hepatocytes from mice fasted for 16 h were treated in 24-well plates (7.5×10^5 cells/well) in buffer A, which consisted of 0.5 mL Krebs-Ringer bicarbonate medium of 119.4 mmol/L NaCl, 3.7 mmol/L KCl, 2.7 mmol/L CaCl₂, 1.3 mmol/L KH₂PO₄, 1.3 mmol/L MgSO₄, and 24.8 mmol/L NaHCO₃ without glucose; 2% (wt/vol) BSA; 0.24 mmol/L 3-isobutyl-1-methylxanthine; and gluconeogenic substrates (1 mmol/L pyruvate plus 10 mmol/L lactate). Hepatocytes were treated with BH₄ (Schircks Laboratories, Jona, Switzerland), sodium nitroprusside (SNP), NG-nitro-L-arginine methyl ester (Sigma, St. Louis, MO), sepiapterin (Schircks Laboratories), erythro-9-(2-hydroxy-3-nonyl)adenine (EHNA) (Wako, Osaka, Japan), and compound C (Sigma). Glucose production was measured by glucose oxidation method as previously described (19).

Immunoblotting analysis of hepatocytes. Western blotting was performed as previously described (19). Primary hepatocytes cultured overnight were incubated in buffer A treated with BH₄, SNP, sepiapterin, and EHNA. Hepatocytes were homogenized in lysis buffer. Cell lysates (50–150 μ g protein/lane) were heated at 95°C for 5 min and subjected to electrophoresis on 6–10% (vol/vol) sodium dodecyl sulfate-polyacrylamide gels and transferred onto nitrocellulose membranes. For analysis of eNOS dimerization, the samples were not heated and the temperature was maintained at <15°C during electrophoresis. Primary antibodies used were anti-phosphorylated (phospho)-AMP kinase (AMPK) α (Thr¹⁷²), anti-AMPK α , anti-phospho-acetyl-CoA carboxylase (ACC) (Ser⁷⁹), anti-ACC, anti-phospho-eNOS (Ser¹¹⁷⁷), anti-phospho-Akt (Ser⁴⁷³), anti-Akt (all at 1:1,000 dilution; Cell Signaling Technology, Danvers, MA), anti-eNOS polyclonal antibody (1:500 dilution; BD Transduction Laboratories, San Jose, CA), anti-CD31 monoclonal antibody (1:2,000 dilution; Dianova, Hamburg, Germany), anti-GTPCH I (1:3,000; kind gift from Prof. H. Ichinose, Tokyo Institute of Technology), anti-dihydrofolate reductase (DHFR), anti- α 1-antitrypsin (1:500; Santa Cruz, Delaware, CA), and anti- β -actin (1:5,000; Sigma). Secondary antibodies used were horseradish peroxidase-conjugated anti-rabbit, -mouse, -rat, or -goat antibody (GE Healthcare, Buckinghamshire, U.K.). The fluorescent bands were visualized using a detection system (Amersham ECL Plus; GE Healthcare) and quantified by densitometry using Image J software from National Institutes of Health (Bethesda, MD).

Cell transfection and short interfering RNA. Stealth short interfering RNA (siRNA) of AMPK α 1 was purchased from Invitrogen (Carlsbad, CA). The sequences of siRNA for AMPK α 1 were 5'-UCUCUUUCCUGAGCCCAUCUU AU-3' and 5'-AUAAGAUGGGUCCUCAGGAAAGAGA-3'. The sequences of control siRNAs were 5'-ACCAACACAGUUUGGGAAUAGGGA-3' and 5'-UCC CUAUCCCCAACUGUUGUUGGU-3'. Isolated hepatocytes in DMEM (low glucose, 5.6 mmol/L) containing 10% (vol/vol) FBS and 100 nmol/L regular insulin were mixed with Opti-MEM containing siRNA and Lipofectamine RNAi MAX (Invitrogen) and were plated on wells and then incubated at 37°C in a CO₂ incubator. The final amounts of hepatocytes, DMEM, Opti-MEM, siRNA, and Lipofectamine RNAi MAX were 5.0×10^5 cells/mL, 75% (vol/vol), 25% (vol/vol), 50 nmol/L, and 0.2%, respectively. Medium was replaced with DMEM 6 h after transfection. Forty-eight hours after transfection, the medium was replaced with buffer A, the cells were incubated for 60 min with or without BH₄, and the glucose content of the supernatant was measured.

Nitrite/nitrate analysis. Primary hepatocytes and liver tissues were homogenized in buffer A, and the amount of nitrite/nitrate in the supernatant was determined by a fluorescence method.

Immunocytochemistry. The hepatocytes were incubated with rabbit polyclonal anti-nitrotyrosine antibody (1:100 dilution; Millipore, Billerica, MA). Cells were then incubated with goat anti-rabbit IgG fluorescein-conjugated secondary antibody (1:100 dilution, Alexa Fluor 488; Invitrogen). Fluorescence in cells was monitored as previously described (19).

Measurement of adenine nucleotide content. After primary isolated hepatocytes were incubated in buffer A with or without BH₄ and SNP for 30 min, treatment was stopped by rapid addition of 0.1 mL of 2 mol/L HClO₄, followed by mixing by vortex and sonication in ice-cold water for 3 min. Adenine nucleotide contents were measured by a luminometric method as previously described (19,20).

Isolation of total RNA and quantitative RT-PCR. Total RNA was isolated from livers of 10 week-old wild-type mice, wild-type mice with STZ-induced diabetes, and *ob/ob* mice using Trizol (Invitrogen) as previously described (21). The mouse sequence of forward and reverse primers to detect GTPCH I and DHFR, glucose 6-phosphatase (G6Pase), phosphoenolpyruvate carboxylase (PEPCK), and glyceraldehyde-3-phosphate dehydrogenase as an inner control are shown in Supplementary Table 1. SYBR Green PCR Master Mix (Applied Biosystems, Foster, CA) was prepared for the quantitative RT-PCR run. The thermal cycling conditions were denaturation at 95°C for 10 min followed by 50 cycles at 95°C for 15 s and 60°C for 1 min. mRNA levels were measured by real-time quantitative RT-PCR using ABI PRISM 7000 Sequence Detection System (Applied Biosystems).

Biopterin analysis. Tissues or whole blood of wild-type mice and wild-type mice with STZ-induced diabetes was collected. For measurement of uptake of BH₄ in liver, BH₄ (20 mg/kg) dissolved with 0.9% (wt/vol) sterile saline was administered intraperitoneally to wild-type mice. After cervical dislocation, the mice were abdominally dissected and liver tissues were collected at 0, 30, 60, 120, and 180 min after injection. The organs were weighed, frozen immediately in liquid N₂, and then stored at -80°C. Total biopterin, BH₄, and BH₂ were measured as previously described (22).

Effect of BH₄ on blood glucose levels of wild-type mice with STZ-induced diabetes, eNOS^{-/-} mice with STZ-induced diabetes, and diabetic Akita mice. Blood glucose levels were measured in wild-type mice with STZ-induced diabetes, eNOS^{-/-} mice with STZ-induced diabetes, and diabetic Akita mice fasted for 16 h, and BH₄ (20 mg/kg) or metformin (250 mg/kg; Sigma) in 0.9% (wt/vol) sterile saline or 0.9% sterile saline alone was injected intraperitoneally. Blood glucose levels were measured again 2 h after injection.

Effect of BH₄ on blood glucose levels of *ob/ob* mice. Blood glucose levels and body weight of *ob/ob* mice were measured. The mice were divided into two groups shown in Supplementary Table 2, and 0.9% (wt/vol) sterile saline with or without BH₄ (10 mg/kg) was injected intraperitoneally twice a day for 10 days. Fed blood glucose levels were measured. After fasting overnight for 16 h, fasting blood glucose levels were measured.

Intraperitoneal glucose tolerance test. Wild-type mice were fasted overnight for 16 h, and glucose (2 g/kg) was injected intraperitoneally with BH₄ (20 mg/kg) in 0.9% (wt/vol) sterile saline or 0.9% sterile saline alone. After 10 days' treatment of saline with or without BH₄ (20 mg/kg), *ob/ob* mice were fasted overnight for 16 h, and glucose (1 g/kg) was injected intraperitoneally. Blood glucose levels and plasma insulin concentrations were measured at 0, 30, 60, 90, and 120 min after injection. Plasma insulin concentrations were determined by using an ELISA kit (Shibayagi, Gunma, Japan). Homeostasis model assessment of insulin resistance (HOMA-IR) was calculated with the following formula: [fasting insulin (mU/L) \times fasting plasma glucose (mmol/L)]/22.5.

Pyruvate tolerance test. Pyruvate, BH₄, and sepiapterin were dissolved with 0.9% (wt/vol) sterile saline. Wild-type, eNOS^{-/-}, and *ob/ob* mice were fasted overnight for 16 h, and pyruvate (1 g/kg) was injected intraperitoneally with or without BH₄ (20 mg/kg) and sepiapterin (20 mg/kg). Blood glucose levels were measured at 0, 30, 60, 90, and 120 min after injection.

Insulin tolerance test. After 10 days' treatment of saline with or without BH₄ (20 mg/kg), *ob/ob* mice were fasted for 6 h, and regular insulin (1 units/kg i.p.) was injected with 0.9% sterile saline. Blood glucose levels were measured at 0, 30, 60, 90, and 120 min after injection.

Statistics. Comparison between two groups was performed using unpaired Student *t* test (not noted) and paired Student *t* test. For more than two groups, one-way or two-way ANOVA followed by post hoc Bonferroni testing was performed. A value of *P* < 0.05 was considered statistically significant.

RESULTS

Biopterin dynamics and effects of BH₄ on blood glucose levels in diabetic mice. In STZ diabetic wild-type mice, the content of BH₂ was increased and the

BH₄-to-BH₂ ratio was decreased in blood and respective tissues (Fig. 1A–D). For investigation of whether BH₄ lowers blood glucose levels, BH₄ (20 mg/kg) in saline was injected intraperitoneally to STZ diabetic wild-type mice. Blood glucose levels were not changed 2 h after administration of BH₄ in fed STZ diabetic wild-type mice, while blood glucose levels were lowered by ~2.4 mmol/L in overnight-fasted STZ diabetic wild-type mice—a change similar to that with metformin (Fig. 1E and F and Supplementary Fig. 1A). The same effects also were found in diabetic Akita mice (Supplementary Fig. 1B).

Liver tissue has an important role in glucose-lowering effects of BH₄. Although the intraperitoneal glucose tolerance test (IPGTT) data in wild-type mice revealed no effects of BH₄ on blood glucose levels and plasma insulin levels, the pyruvate tolerance test (PTT) data showed that BH₄ decreased hepatic glucose production (Fig. 2A–C), suggesting that the suppressing effect on hepatic gluconeogenesis has a critical role in the glucose-lowering effect

of BH₄. The mRNA and protein expression levels of GTPCH I, a rate-limiting enzyme of the BH₄ de novo synthesis pathway, were decreased in liver tissues of STZ diabetic wild-type mice (Fig. 2D and E). On the other hand, uptake of BH₄ into liver by its supplementation is regulated by DHFR, a rate-limiting enzyme of the BH₄ salvage synthesis pathway (23), and the expression of DHFR in liver tissues of STZ diabetic wild-type mice was not changed (Fig. 2F and G). The uptake of BH₄ in liver of wild-type mice was confirmed with a peak at 30 min by administration of BH₄ (20 mg/kg) as previously described (22,23) (Supplementary Fig. 2A). After 2-h administration of BH₄, the mRNA expression levels of PEPCK were significantly decreased, while those of G6Pase were not changed, and the eNOS dimerization and NO content were increased in the liver of STZ diabetic wild-type mice (Fig. 2H–K). The mRNA expression levels of PEPCK and G6Pase in the liver of wild-type mice were not changed (Supplementary Fig. 2B and C).

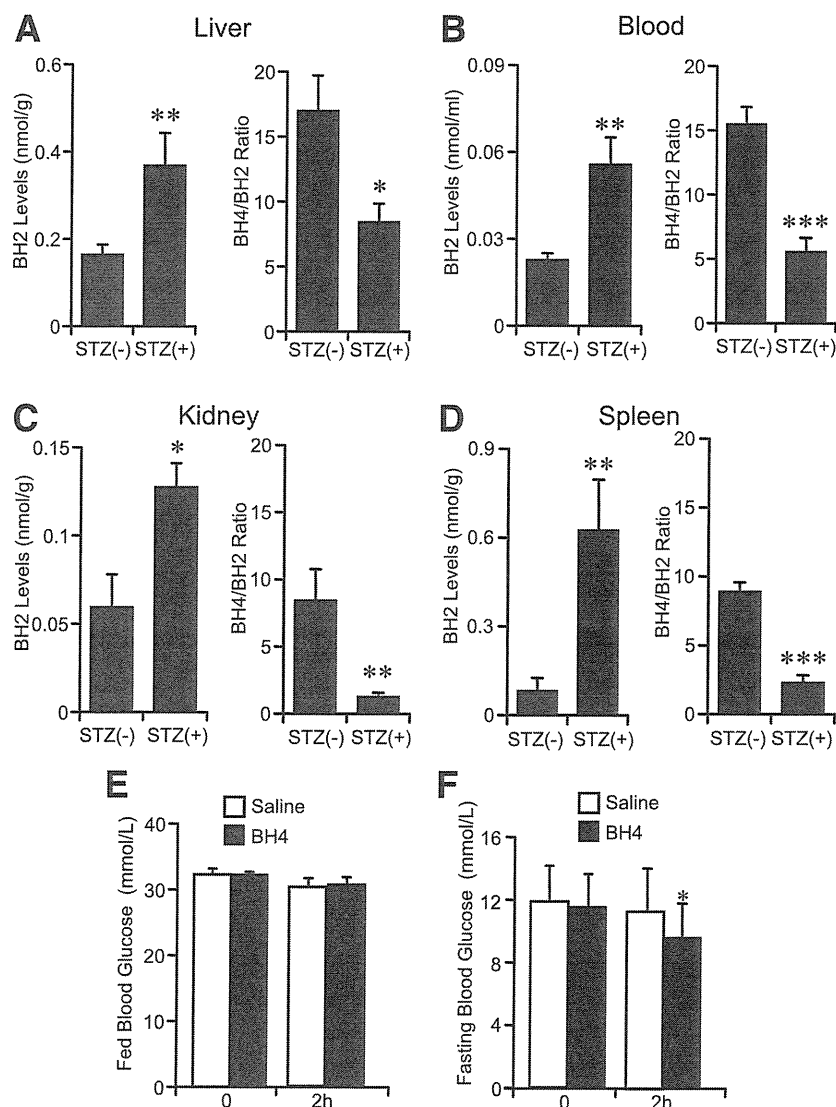


FIG. 1. Biotpterin dynamics and effects of BH₄ on blood glucose levels in diabetic mice. A–D: BH₂ levels and BH₄-to-BH₂ ratio of liver, blood, kidney, and spleen. Values are means \pm SE. $n = 7$. * $P < 0.05$, ** $P < 0.01$, *** $P < 0.001$ vs. without STZ. E and F: Fed blood glucose levels were not changed 2 h after injection of BH₄ (20 mg/kg i.p.) to STZ diabetic wild-type mice; fasting blood glucose levels were significantly decreased. Values are means \pm SE. $n = 8$. * $P < 0.05$ vs. the value of preinjection of saline with BH₄ intraperitoneally; paired t test. No significant difference of fed and fasting blood glucose levels 2 h after intraperitoneal injection of saline to mice with STZ-induced diabetes.

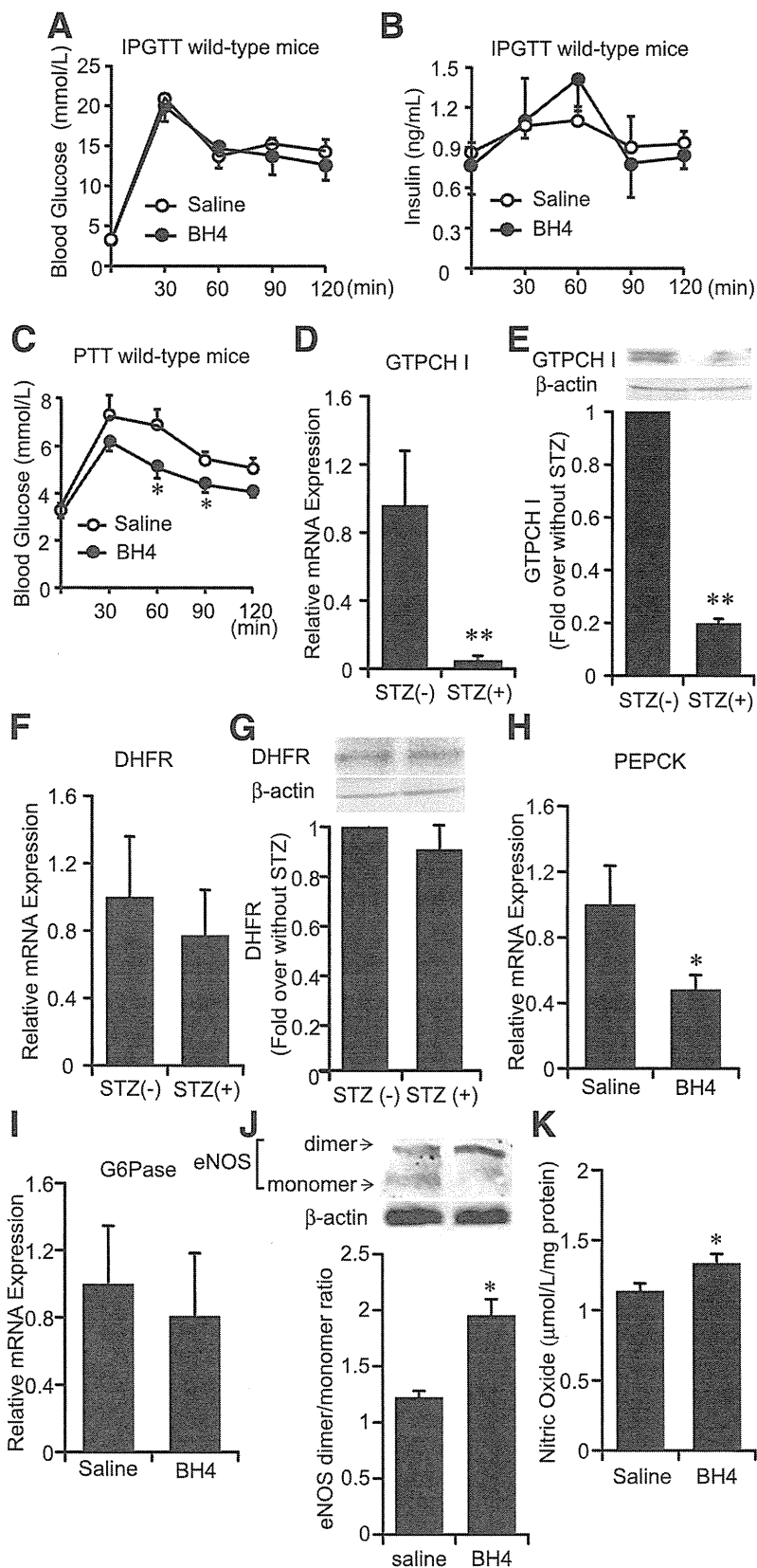


FIG. 2. Role of liver tissue in glucose-lowering effects of BH₄. **A** and **B**: IPGTT to wild-type mice. Blood glucose levels and plasma insulin levels after administration of glucose (2 g/kg i.p.) with or without BH₄ (20 mg/kg). Values are means ± SE (n = 6). **C**: PTT to wild-type mice. Elevation of blood glucose levels after intraperitoneal administration of pyruvate with BH₄ (20 mg/kg) to wild-type mice was suppressed compared with those without BH₄. Values are means ± SE (n = 6). *P < 0.05 vs. saline. **D**: In mice with STZ-induced diabetes, mRNA levels of GTPCH I expression were significantly decreased compared with those in nondiabetic wild-type mice liver. Values are means ± SE (n = 5). **P < 0.01 vs. nondiabetic wild-type mice liver. **E**: In wild-type mice with STZ-induced diabetes, protein expression levels of GTPCH I were significantly decreased compared with those in nondiabetic wild-type mice liver. Values are means ± SE (n = 5). **P < 0.01 vs. nondiabetic wild-type mice liver. **F**: No significant difference

BH₄ suppresses gluconeogenesis and increases AMPK α phosphorylation in wild-type mouse hepatocytes. As eNOS expression was confirmed in isolated hepatocytes from wild-type mice (Supplementary Fig. 3), we examined the direct effect of BH₄ in suppression of hepatic gluconeogenesis using hepatocytes isolated from wild-type mice fasted for 16 h. In a time course study of exposure to BH₄, the suppressing effect on gluconeogenesis appeared after 60 min ($P < 0.01$ vs. corresponding control) (Fig. 3A). We then investigated the increment of AMPK α phosphorylation by time course exposure of BH₄ to hepatocytes. AMPK was activated after 30 min by BH₄ (Fig. 3B). After 60 min exposure to BH₄, gluconeogenesis was dose-dependently suppressed at doses of 50 and 100 $\mu\text{mol/L}$ BH₄ (control, 101.7 ± 3.7 nmol/mg protein; 50 $\mu\text{mol/L}$ BH₄, 72.4 ± 7.1 nmol/mg protein, $P < 0.01$ vs. control; 100 $\mu\text{mol/L}$ BH₄, 60.6 ± 4.1 nmol/mg protein, $P < 0.001$ vs. control) (Fig. 3C). AMPK was activated at doses of 50 and 100 $\mu\text{mol/L}$ BH₄ by 30 min exposure (Fig. 3D). In accordance with the activation of AMPK, an increase in phosphorylation of ACC by BH₄ was confirmed (Fig. 3B and D). For determination of whether BH₄ suppresses gluconeogenesis in an AMPK-dependent manner, the effect of silencing AMPK was examined (Fig. 3E). By transfection of AMPK α 1 siRNA, the suppressing effect of BH₄ on gluconeogenesis disappeared (Fig. 3F). The suppressing effect of BH₄ on gluconeogenesis also disappeared in the presence of compound C, an AMPK inhibitor (Fig. 3G).

BH₄ suppresses gluconeogenesis and increases AMPK α phosphorylation eNOS dependently in hepatocytes. Exposure to BH₄ in hepatocytes increased NO production and eNOS phosphorylation (Fig. 4A and B). To examine whether BH₄ suppresses hepatic gluconeogenesis and activates AMPK in the absence of eNOS, we performed experiments using mouse hepatocytes lacking eNOS. In hepatocytes isolated from eNOS^{-/-} mice, BH₄ did not suppress gluconeogenesis (control, 103.9 ± 10.8 nmol/mg protein; 50 $\mu\text{mol/L}$ BH₄, 98.5 ± 11.3 nmol/mg protein; 100 $\mu\text{mol/L}$ BH₄, 89.1 ± 10.9 nmol/mg protein, $P = \text{NS}$ vs. control) (Fig. 4C). BH₄ did not alter AMPK α and ACC phosphorylation in hepatocytes lacking eNOS (Fig. 4D). The suppressing effect of BH₄ on gluconeogenesis and activation of AMPK also disappeared in the presence of NG-nitro-L-arginine methyl ester, an NOS inhibitor (Supplementary Fig. 4A and B). SNP, an NO donor, has suppressing effects on gluconeogenesis and increases the effects on AMPK activation both in wild-type and eNOS^{-/-} hepatocytes (Supplementary Fig. 5A–D). Immunocytochemical staining of primary cultured hepatocytes from wild-type mice with anti-nitrotyrosine antibody, which detects ONOO⁻, showed that ONOO⁻ production was not increased by exposure with BH₄ or SNP (Supplementary Fig. 5E).

Effect of BH₄ on adenine nucleotide content in hepatocytes. For investigation of the mechanism of AMPK activation by BH₄ in hepatocytes, the adenine nucleotide content with exposure of BH₄ to hepatocytes was measured. BH₄ and SNP significantly increased AMP content in wild-type mouse hepatocytes (Table 1). Unexpectedly,

BH₄ also significantly increased ATP content. To clarify the mechanism by which BH₄ increases AMP content and activates AMPK in hepatocytes, we examined the effect of AMP deaminase (AMPD) on activation of AMPK and suppression of gluconeogenesis by BH₄. Although EHNA, a known AMPD inhibitor, activated AMPK and suppressed hepatic gluconeogenesis, BH₄ did not have an additive effect on EHNA (Supplementary Fig. 6A and B). These results indicate that inhibition of AMPD, at least in part, contributes to AMP accumulation by BH₄ in hepatocytes. **Sepiapterin, a BH₄ precursor, suppresses gluconeogenesis and increases AMPK activation.** Similarly to BH₄, sepiapterin is absorbed in hepatocytes and immediately converted to BH₄ via a salvage pathway of BH₄ biosynthesis (23). Sepiapterin was found to suppress gluconeogenesis and activate AMPK (Fig. 5A and B). However, these effects were abolished in hepatocytes lacking eNOS (Fig. 5A and B).

Role of eNOS in in vivo action of BH₄ on glucose metabolism. The lowering effect of BH₄ on fasting blood glucose levels disappeared in STZ-induced diabetic eNOS^{-/-} mice (Fig. 6A). The PTT data showed that BH₄ did not decrease hepatic glucose production in eNOS^{-/-} mice (Fig. 6B). Similar results were also obtained in sepiapterin administration (Supplementary Fig. 7A and B). We then compared the effects of BH₄ on phosphorylation of AMPK α in liver tissues of these diabetic mice. BH₄ activated AMPK in both STZ diabetic wild-type mice liver and diabetic Akita mice liver but not in STZ diabetic eNOS^{-/-} mice liver (Fig. 6C and D and Supplementary Fig. 8A). AMPK α phosphorylation was not changed by fasting for 16 h in liver tissues of wild-type mice (Supplementary Fig. 8B).

Effects of BH₄ on glucose metabolism and insulin sensitivity in ob/ob mice. Our PTT data show that the suppressing effect on gluconeogenesis is also confirmed by single administration of BH₄ in ob/ob mice (Fig. 7A), while the mRNA expression levels of PEPCK and G6Pase in the liver (Supplementary Fig. 9A and B), fasting and fed blood glucose levels, and IPGTT data were not changed (data not shown). By consecutive administration of BH₄ (20 mg/kg) in saline for 10 days to ob/ob mice, fasting blood glucose levels were significantly lowered by 3.9 mmol/L and fed blood glucose levels tended to be decreased compared with those in ob/ob mice treated with saline alone (Fig. 7B and C). Our IPGTT, HOMA-IR, and insulin tolerance test data suggest that consecutive administration of BH₄ ameliorates glucose intolerance as well as insulin resistance (Fig. 7D–G). Phosphorylation of AMPK α , ACC, and Akt was increased in liver tissues of BH₄-treated ob/ob mice compared with those in saline-treated mice (Fig. 7H and I).

DISCUSSION

The current study shows that BH₄, known as a cofactor of eNOS, has a glucose-lowering effect in diabetic mice. The BH₄-to-BH₂ ratio was found to be decreased in various tissues of mice in the diabetic state, indicating deterioration of

of mRNA expression levels of DHFR in liver was detected between nondiabetic mice and mice with STZ-induced diabetes. Values are means \pm SE ($n = 10$). G: No significant difference of protein expression levels of DHFR in liver was detected between nondiabetic mice and mice with STZ-induced diabetes. Values are means \pm SE ($n = 5$). H and I: In liver tissues of wild-type mice with STZ-induced diabetes treated with BH₄, mRNA levels of PEPCK were significantly decreased compared with those treated without BH₄. The mRNA levels of G6Pase were not changed. Values are means \pm SE ($n = 6$), * $P < 0.05$ vs. saline. J: Liver tissues of eNOS dimer and monomer expression 2 h after intraperitoneal injection of saline with or without BH₄ (20 mg/kg) to wild-type mice with STZ-induced diabetes. Densitometric analysis of the ratio of eNOS dimer to monomer. Values are means \pm SE ($n = 5$). * $P < 0.05$ vs. saline. K: In liver tissues of wild-type mice with STZ-induced diabetes treated with BH₄, NO content was significantly increased compared with those treated without BH₄. Values are means \pm SE ($n = 5$). * $P < 0.05$ vs. saline.

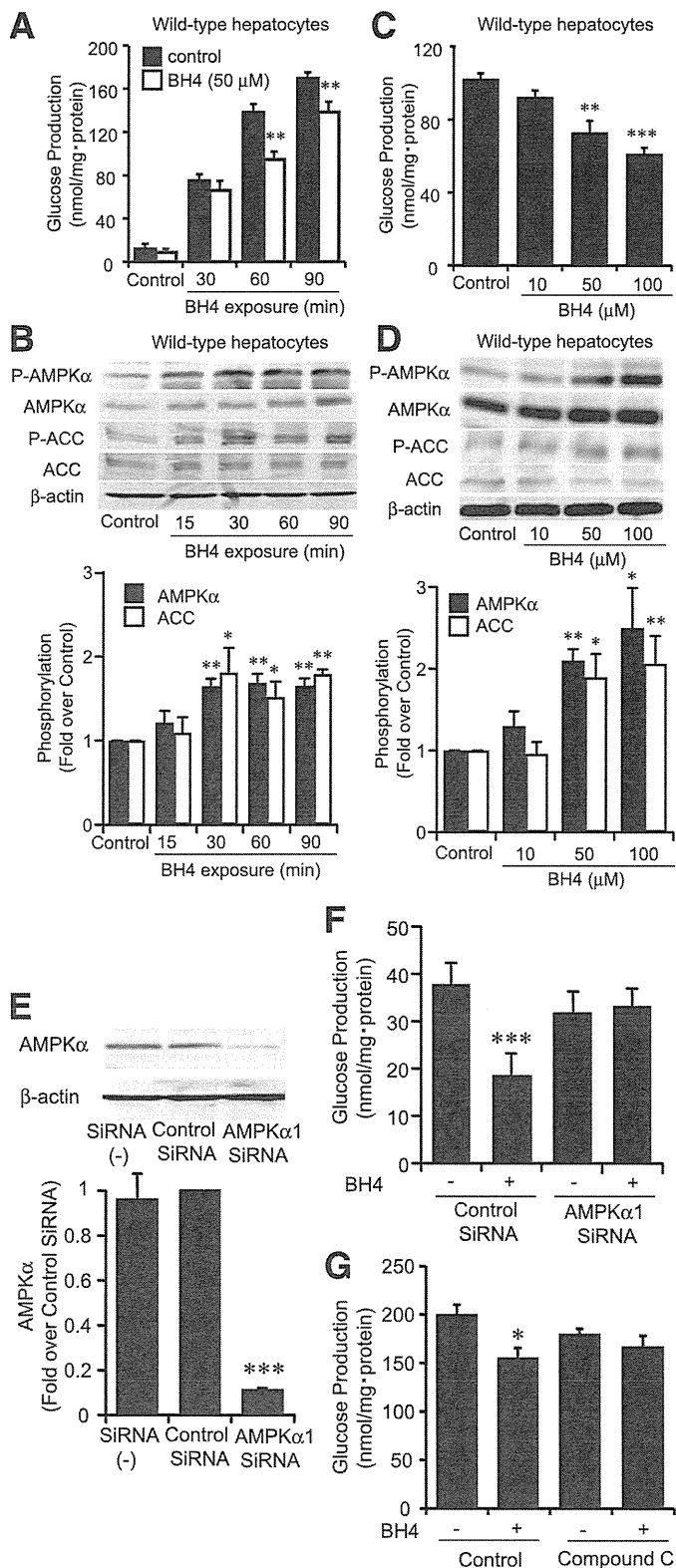


FIG. 3. BH₄ suppressed gluconeogenesis and increased AMPKα phosphorylation in hepatocytes isolated from wild-type mice. **A:** Time course of gluconeogenesis by 50 μmol/L BH₄ compared with control was detected after 60 min in hepatocytes isolated from wild-type mice. Values are means ± SE (n = 6). **P < 0.01 vs. control. **B:** Time course of phosphorylation of AMPKα and ACC upon exposure to BH₄ (50 μmol/L). Both AMPKα and ACC phosphorylation were stimulated after 30 min exposure to BH₄ in hepatocytes isolated from wild-type mice. Data are expressed as fold stimulation over control. Values are means ± SE (n = 3). *P < 0.05, **P < 0.01 vs. control. **C:** Suppressing effect on

eNOS bioactivity by eNOS uncoupling. Previous studies have shown that impairment of eNOS function is involved in glucose dysmetabolism and insulin resistance (4,5), which lends support to the notion that alleviation of eNOS dysfunction such as by supplementation of BH₄ ameliorates glucose dysmetabolism and insulin resistance. In addition, we found that supplementation of BH₄ increased dimerization of eNOS and NO production in the liver of diabetic mice, which strongly suggests alleviation of eNOS dysfunction by recoupling of eNOS. Simultaneously with the restoration of eNOS activity, BH₄ elicited a glucose-lowering effect in these mice. No such glucose-lowering effect by BH₄ appeared in diabetic mice lacking eNOS. These findings clearly implicate recoupling of eNOS in the glucose-lowering effect of BH₄.

We have shown that the liver plays a critical role in the glucose-lowering effect of BH₄ through suppression of hepatic gluconeogenesis. It is well-known that BH₄ is synthesized mainly in liver (24) and that this is impaired by oxidative stress such as liver cirrhosis and diabetes (25,26). Single administration of BH₄ is known to accumulate at higher levels in liver than other tissues including skeletal muscle (24), which also lends support to the view that BH₄ readily elevates BH₄-to-BH₂ ratio and regulates glucose metabolism in the liver.

We then investigated the molecular mechanism of suppression of hepatic gluconeogenesis by BH₄ using isolated mouse hepatocytes. BH₄ acts directly on hepatocytes and suppresses hepatic gluconeogenesis eNOS dependently. Several studies reported that eNOS is found in hepatic sinusoidal and venous endothelial cells and not in hepatocytes (27,28), whereas other studies claim detection of eNOS in hepatocytes (29,30). We confirmed that eNOS is expressed in hepatocytes, which suggests that intra-hepatocellular eNOS is essential for the effect of BH₄ in suppression of hepatic gluconeogenesis. In addition, BH₄ activated AMPK, and the suppressing effect of BH₄ on gluconeogenesis disappeared by siRNA silencing of AMPKα1 subunits in hepatocytes, indicating that AMPK is involved in the suppressing effect of BH₄ on hepatic gluconeogenesis. AMPK activation by BH₄ was not observed in eNOS^{-/-} mouse hepatocytes or in the presence of NOS inhibitor, suggesting that eNOS acts upstream of AMPK activation in suppression of hepatic gluconeogenesis by BH₄. AMPK is a Ser/Thr kinase that acts as an energy sensor and is activated by an increase in the AMP-to-ATP ratio and/or AMP in response to a variety of metabolic stresses, such as hypoxia, ischemia, and exercise (31,32). In our data, BH₄ significantly increased AMP content and

gluconeogenesis after 1 h exposure of BH₄ was detected ranging over 50 μmol/L in hepatocytes isolated from wild-type mice. Values are means ± SE (n = 6). **P < 0.01, ***P < 0.001 vs. control. **D:** Effect of BH₄ on phosphorylation of AMPK and ACC. After 30 min exposure to BH₄, both AMPKα and ACC phosphorylation were increased by BH₄ dose dependently ranging over 50 μmol/L in hepatocytes isolated from wild-type mice. Data are expressed as fold stimulation over control. Values are means ± SE (n = 3). *P < 0.05, **P < 0.01 vs. control. **E:** With transfection with AMPKα1 siRNA, protein expression of AMPKα was decreased compared with that of transfection with control siRNA. Values are means ± SE (n = 3). ***P < 0.001 vs. control siRNA. **F:** Transfected with AMPKα1 siRNA, suppressing effect of BH₄ (50 μmol/L) on hepatic glucose production was inhibited. Values are means ± SE (n = 6). ***P < 0.001 vs. values transfected with control siRNA without BH₄. **G:** Compound C (20 μmol/L), an AMPK inhibitor, abolished the suppressing effect of BH₄ (50 μmol/L) on gluconeogenesis. Values are means ± SE (n = 6). *P < 0.05 vs. values without BH₄ and without compound C.

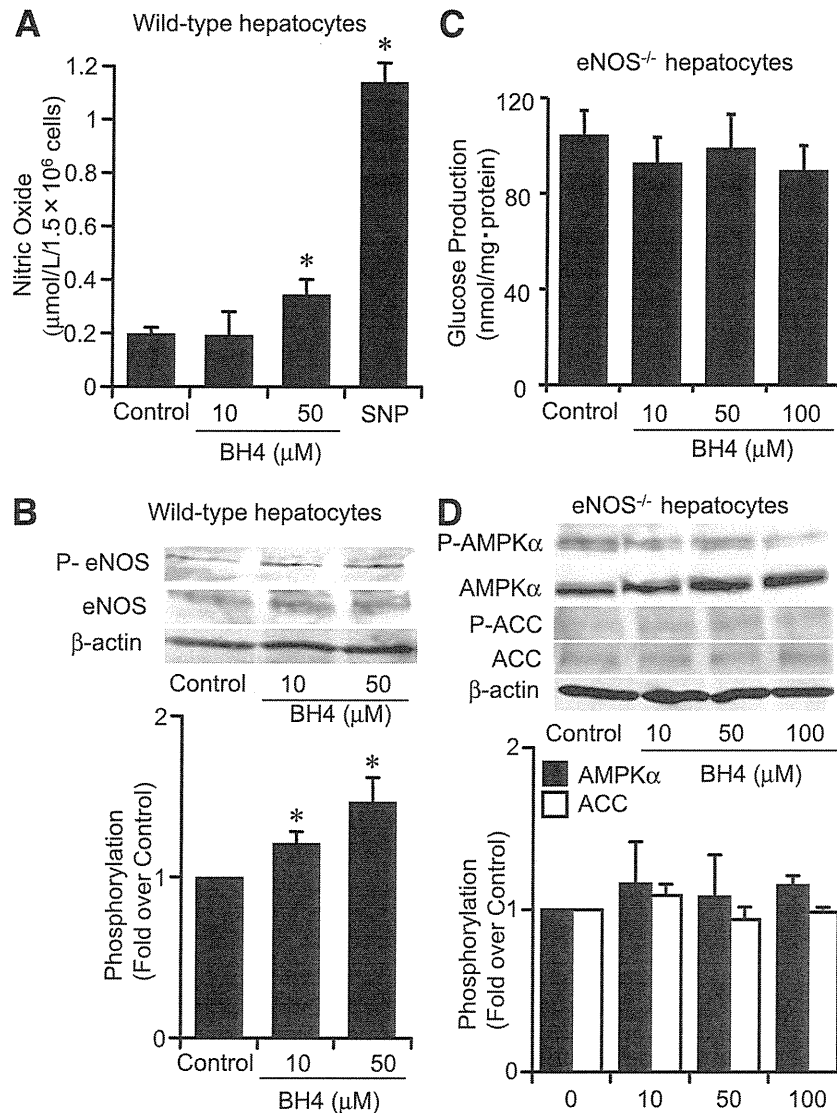


FIG. 4. Lack of the effect of BH₄ on suppression of gluconeogenesis in eNOS^{-/-} mouse hepatocytes. **A:** BH₄ (50 μmol/L) significantly increased NO production in hepatocytes from wild-type mice. SNP (20 μmol/L) was used as positive control. Values are means ± SE (*n* = 5). **P* < 0.05 vs. control. **B:** BH₄ (ranging from 10 to 50 μmol/L) increased eNOS phosphorylation at Ser¹¹⁷⁷ in hepatocytes from wild-type mice. Values are means ± SE (*n* = 5). **P* < 0.05 vs. control. **C:** BH₄ (ranging from 10 to 100 μmol/L) did not suppress gluconeogenesis after 1 h exposure in hepatocytes from eNOS^{-/-} mice. Values are means ± SE (*n* = 6). **D:** After 30 min exposure to BH₄ ranging from 10 to 100 μmol/L, AMPKα and ACC phosphorylation were not increased by BH₄ in hepatocytes from eNOS^{-/-} mice. Data are expressed as fold stimulation over control. Values are means ± SE (*n* = 3).

tended to increase the AMP-to-ATP ratio. It is known that inhibition of AMPD increases AMP in isolated hepatocytes (33). Recently, Ouyang et al. (34) reported that inhibition of AMPD might be involved in increased production of

TABLE 1
Effects of BH₄ on ATP, AMP, and AMP-to-ATP ratio in wild-type mouse hepatocytes

	ATP (nmol/mg protein)	AMP (nmol/mg protein)	AMP-to-ATP ratio
Control	0.66 ± 0.08	0.28 ± 0.04	0.44 ± 0.03
BH ₄	0.88 ± 0.04*	0.49 ± 0.05**	0.55 ± 0.04
SNP	0.73 ± 0.07	0.47 ± 0.01**	0.67 ± 0.07

Data are means ± SE (*n* = 5). Hepatocytes were incubated in Krebs-Ringer bicarbonate buffer with or without BH₄ (50 μmol/L) for 30 min. The treatment was stopped by rapid addition of 0.1 mL of 2 mol/L HClO₄, and adenine nucleotide contents were measured. **P* < 0.05, ***P* < 0.01 vs. control.

AMP and activation of AMPK by metformin. In the current study, the AMPD inhibitor EHNA was found to activate AMPK, but BH₄ did not elicit an additional effect on AMPK activation in the presence of EHNA, suggesting that AMPD might be inhibited by BH₄ in hepatocytes. Interestingly, BH₄ significantly increased ATP content along with the increase in AMP. This effect was not found in exposure to other potent AMPK activators, as previously reported (35). The reason why BH₄ increases ATP content is unclear, but BH₄ is known to work as an antioxidant (36). It has been reported that BH₄ preserves ATP content and has a cytoprotective effect from hypoxia on neuronal cells (37). BH₄ might thus prevent cytotoxic damage from reactive oxygen species/reactive nitrogen species (RNS) as a scavenger, keeping ATP content higher than in the absence of BH₄. We therefore cannot exclude the possibility that BH₄ acts as a reactive oxygen species/RNS scavenger in ameliorating glucose dysmetabolism, but such an effect would be limited in terms of suppressing hepatic gluconeogenesis

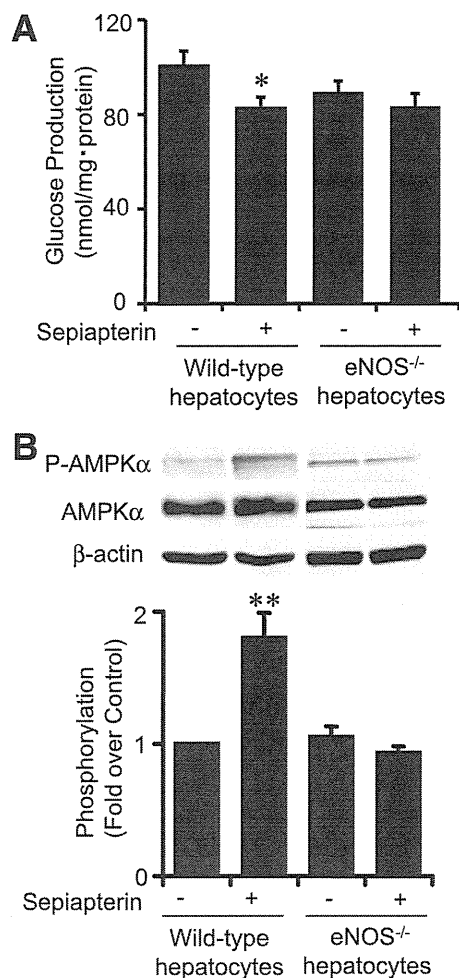


FIG. 5. Effect of sepiapterin, a BH₄ precursor, on gluconeogenesis and AMPK activation. **A:** After 1 h exposure, sepiapterin (50 μmol/L) significantly suppressed gluconeogenesis in hepatocytes isolated from wild-type mice. This effect was not observed in hepatocytes isolated from eNOS^{-/-} mice. Values are means ± SE (*n* = 6). **P* < 0.05 vs. control. **B:** After 30 min exposure to sepiapterin (50 μmol/L), AMPKα phosphorylation was increased in hepatocytes isolated from wild-type mice. AMPKα phosphorylation was not increased by sepiapterin in hepatocytes isolated from eNOS^{-/-} mice. Data are expressed as fold stimulation over control. Values are means ± SE (*n* = 3). ***P* < 0.01 vs. control.

because the effect of BH₄ was not observed in mice lacking eNOS. Previous studies found that NO has an activating effect on AMPK (38,39). Also, in our results SNP, an NO donor, activated AMPK in hepatocytes just as BH₄ does. Regarding the mechanism of AMPK activation by BH₄ via eNOS, it is possible that NO itself generated by eNOS activates AMPK; another possibility is that the RNS peroxynitrite (ONOO⁻), an adduct of NO with superoxide, works intermediately as the activator of AMPK by BH₄ (19,40). The involvement of RNS on AMPK activation by BH₄ was not suggested by our present data.

Our data using *ob/ob* mice, a mouse model of insulin resistance, suggest that the primary physiological action of BH₄ is a suppressing effect of hepatic gluconeogenesis. In addition to this effect, consecutive administration of BH₄ ameliorated glucose intolerance as well as insulin resistance. A possible mechanism of these additive effects of BH₄ is induction by the subsequent downstream targets of AMPK activated by BH₄ such as metformin, which are known to have insulin-sensitizing effects, e.g., by

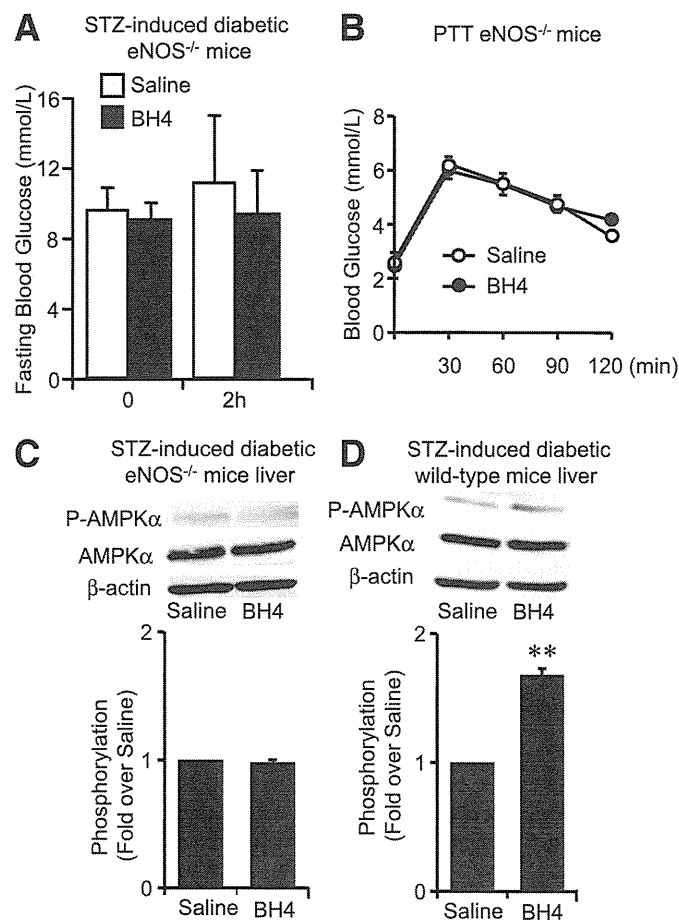


FIG. 6. Effects of BH₄ in eNOS^{-/-} mice with STZ-induced diabetes. **A:** No significant difference of fasting blood glucose levels 2 h after intraperitoneal injection of saline with or without BH₄ (20 mg/kg) to eNOS^{-/-} mice with STZ-induced diabetes. Values are means ± SE (*n* = 7). **B:** PTT to eNOS^{-/-} mice. No effects of BH₄ (20 mg/kg) on suppressing hepatic gluconeogenesis were detected in PTT in eNOS^{-/-} mice. Values are means ± SE (*n* = 6). **C:** AMPKα phosphorylation in liver of eNOS^{-/-} mice with STZ-induced diabetes was not changed by BH₄ administration. Data are expressed as fold stimulation over saline. Values are means ± SE (*n* = 3). **D:** AMPKα phosphorylation in liver of wild-type mice with STZ-induced diabetes was significantly increased by BH₄ (20 mg/kg) administration. Data are expressed as fold stimulation over saline. Values are means ± SE (*n* = 3). ***P* < 0.01 vs. saline.

modulating carbohydrate and lipid metabolism via the downstream signals of AMPK (41). It is generally known that increase in Akt phosphorylation represents an amelioration of hepatic insulin resistance. This may be applicable to the effect of BH₄, while it raises the possibility that Akt-dependent signaling is involved in the suppressing effect of BH₄ on hepatic gluconeogenesis in *ob/ob* mice. Another possible mechanism of BH₄ ameliorating insulin resistance would be via a direct effect of BH₄ on endothelial cells. Similar to several NO donors and NO-moderating compounds (42), BH₄ might also exert an insulin-sensitizing effect by augmenting the delivery of insulin and glucose to skeletal muscle via capillary recruitment. Since the role of eNOS in vivo was assessed using global eNOS^{-/-} mice, it is difficult to exclude the possibility of indirect effects of eNOS on the liver. Therefore, limitations of the current study must be considered. Further investigations, e.g., by using liver-specific eNOS^{-/-} mice, are required to elucidate the pleiotropic effects of BH₄ in lowering blood glucose levels.